X-625-73-78
PREPRINT

BEHAVIOR OF NITRIC OXIDE FORMED BY THE SPACE SHUTTLE IN THE MESOSPHERE

IGOR J. EBERSTEIN
A. C. AIKIN

MARCH 1973

GSFC — GODDARD SPACE FLIGHT CENTER
GREENBELT, MARYLAND

BEHAVIOR OF NITRIC OXIDE DEPOSITED BY THE SPACE SHUTTLE IN THE MESOSPHERE

by

Igor J. Eberstein
Consultants and Designers
Greenbelt, Maryland

and

A. C. Aikin
Laboratory for Planetary Atmospheres
NASA/Goddard Space Flight Center
Greenbelt, Maryland

TABLE OF CONTENTS

ABSTRACT

Reentry of the space shuttle in the altitude region between 85 km and 70 km is expected to convert 1% to 10% of the intercepted air stream into nitric oxide. Most of the nitric oxide will be concentrated in a wake of small initial radius. The early, highly turbulent part of the trail will rapidly diffuse the initial high concentration of nitric oxide. As wake turbulence decays, atmospheric mixing processes become dominant and further decreases in contaminant concentration are slower. Atmospheric mixing is assumed to become dominant at a nitric oxide centerline concentration of 2×10^{12} molecules/cc. Starting with these conditions a numerical model of eddy diffusive transport of emitted gases from the space shuttle wake, including chemical reactions between the emitted constituents and the ambient atmosphere, has been constructed for 75 km altitude. The numerical methods involve explicit solution of the diffusion equation and Runge-Kutta method for the chemical reactions. The time required to reach background levels of nitric oxide concentration of 7×10^{7} molecules/cc has been calculated. This relaxation time depends strongly on atmospheric conditions. Dissipation takes only a few hours when strong winds and a high level of turbulence prevail, while decay times in a quiescent atmosphere are measured in weeks. As the wake expands, atmospheric ozone interacts with nitric oxide to give molecular oxygen and

nitrogen dioxide. The ozone depletion in the surroundings of the wake results in a "hole" where ozone concentration is less than 50% of the normal background of 10^{10} molecules/cc. For a quiescent atmosphere, this ozone hole reaches a maximum extent in four hours, and collapses again in less than twelve hours. At its maximum, the hole is one kilometer wide and 300 meters thick, with a length of thousands of kilometers. Normally, strong wind shears are expected. These have been shown to significantly increase the rate of dispersion of the trail. The preliminary conclusion is that transient effects on atmospheric ozone are not very serious. However, it is recommended that the present computations be expanded to include typical entry trajectories, considered necessary because eddy diffusivity, wind shear, and atmospheric chemistry are all altitude dependent. The effect of enhanced ionization resulting from photoionization of the wake should also be computed. Potential accummulation of nitric oxide in the mesosphere and stratosphere over time periods of several years at projected levels of operation should also be studied.

INTRODUCTION

A spacecraft such as the space shuttle entering the Earth's atmosphere dissipates a large percentage of its orbital energy between 85 and 70 kilometer altitude. Some of this energy results in the dissociation of molecular oxygen and nitrogen and the formation of nitric oxide, which is contained in a trail of small initial radius e.g. 7.6 meters. The length of the trail may be as much as 6000 kilometers. The quantity of nitric oxide formed depends on several factors including spacecraft angle of attack, weight and surface area and can be as great as 10% of the air swept by the vehicle. This can lead to initial concentrations as great as 10^{14} molecules/cc at 75 km. A discussion of this problem can be found in a report by Park (1972). Park estimated that shuttle flight operations will produce 950,000 pounds (432,000 kg) of NO per year. If this were to remain in a shell, 1 km thick at 75 km, then the background NO concentration would be increased by 7×10^{7} molecules/cc which doubles the background.

The concentration of nitric oxide confined within the initial tube of air intercepted by the vehicle can be as much as 6 orders of magnitude above the average background density of mesospheric nitric oxide. Such large concentrations will be reduced initially by rapid mixing in the high

velocity near wake. However, the total time required to reach the background density depends on many factors incldding the rate of diffusion, chemical reactions and wind shear.

In this report a numerical model of eddy-diffusive transport of gases in the "persistent" space shuttle wake is constructed. Chemical reactions between nitric oxide and the ambient atmosphere are included. The numerical methods involve explicit solution of the diffusion equation and the Runge-Kutta or Euler method for chemical reactions.

Three forms of diffusive behavior are investigated, namely one dimensional, axisymmetric, and two dimensional. By the latter is meant a situation were vertical and horizontal diffusion coefficients are significantly different, but both finite. The effect of wind shear is considered from some of the two dimensional cases.

The chemistry is complex and it is recognized that many of the reactions that take place in the immediate vicinity of the vehicle where the air temperature is high do not occur in the ambient atmosphere. The next section deals with the chemistry and describes the reactions that have been included in the diffusion computations.

CHEMICAL PROCESSES AFFECTING THE NO DISTRIBUTION

As a nitric oxide trail expands in the mesosphere, it undergoes several photochemical processes. Reactions of importance are listed in Table I and include photodissociation,

reaction with atomic nitrogen and oxygen as well as the important interaction with ozone namely

$$NO + O_3 \rightarrow NO_2 + O_2$$

This reaction depletes atmospheric ozone by converting it to molecular oxygen. The effect on the ambient ozone distribution will be large whenever nitric oxide significantly exceeds ozone. This is illustrated in Figure 1 where the ozone computed at 75 km for a nitrogen-oxygen atmosphere is given diurnally for different initial NO concentrations. In the real case the nitric oxide concentration is decreasing with time at a given location due to diffusion. Also the reentry body has initially destroyed all ozone in the region where NO is produced. As will be shown, this "ozone hole" expands with trail radius, as ozone reacts with NO to form NO_2.

ONE DIMENSIONAL DIFFUSION

The diffusion equation is given as follows for one dimension:

$$\frac{\partial c}{\partial t'} = D \frac{\partial^2 c}{\partial x^2} \qquad (1)$$

where c is concentration, t' is time, x is distance, and D is the molecular or eddy diffusion coefficient. In the above formulation it has been implicity assumed that D is a weak function of time and space, i.e.

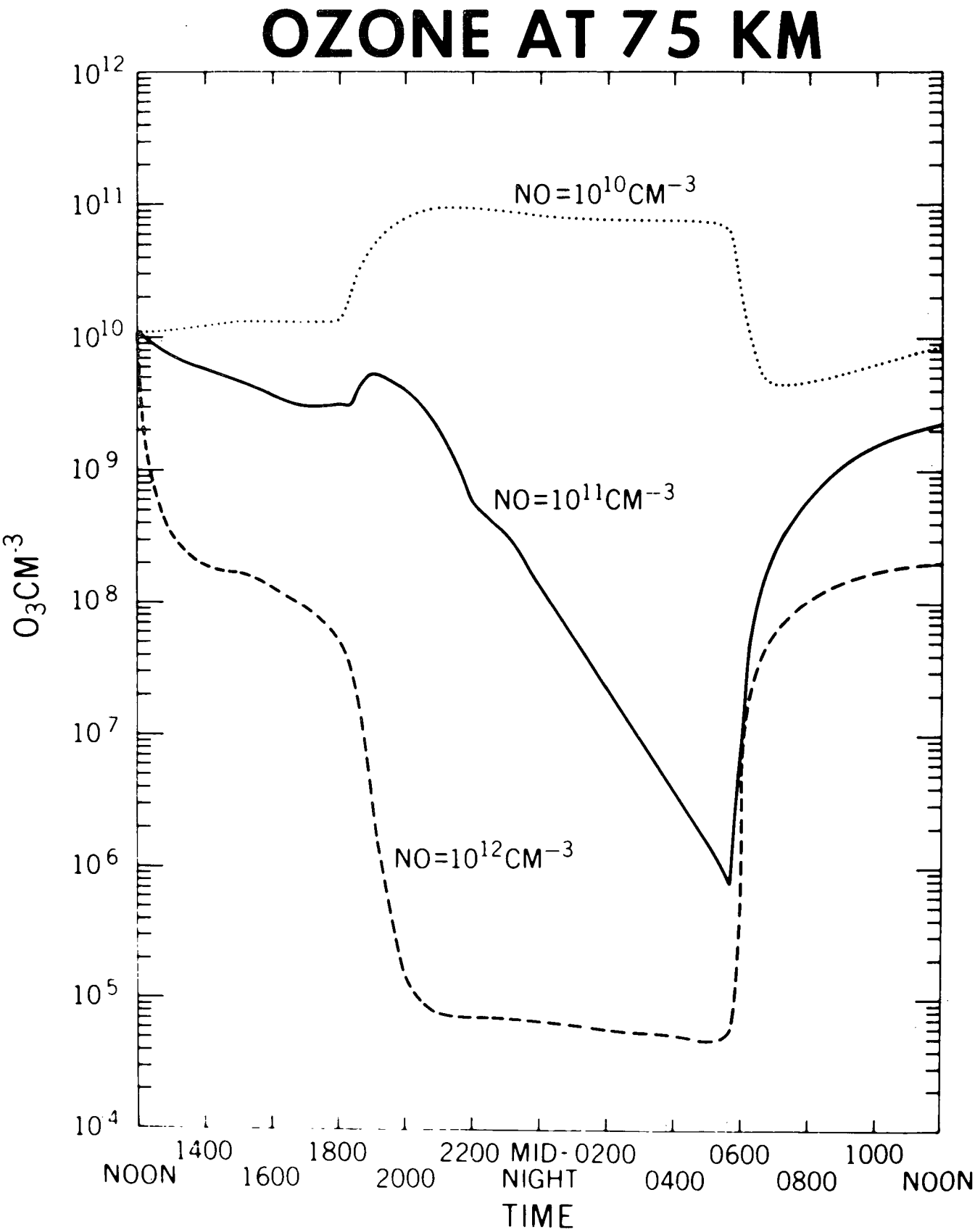
OZONE AT 75 KM
10^{12}
10^{11}
10^{10}
10^{9}
10^{8}
10^{7}
10^{6}
10^{5}
10^{4}
O_3CM^{-3}
NO=10^{10}CM^{-3}
NO=10^{11}CM^{-3}
NO=10^{12}CM^{-3}
NOON
1400
1600
1800
2000
2200
MID-NIGHT
0200
0400
0600
0800
1000
NOON
TIME

$$\left|\frac{\partial D}{\partial x}\right| \ll 1$$

$$\left|\frac{\partial D}{\partial t'}\right| \ll 1 \qquad (2)$$

Now, define

$$t \equiv t'D \qquad (3)$$

Since $\frac{\partial}{\partial t} = \frac{1}{D}\frac{\partial}{\partial t'}$ we obtain the dimensionless diffusion equation:

$$\frac{\partial c}{\partial t} = \frac{\partial^2 c}{\partial x^2} \qquad (4)$$

The solution of the above equation as an initial value problem is given by Courant and Hilbert (1968) as follows:

$$U(x,t) = \frac{1}{2\sqrt{\pi t}} \int_{-\infty}^{+\infty} \psi(\xi)\, \exp(-(x-\xi)^2/4t)\, d\xi \qquad (5)$$

where $\psi(\xi)$ is the distribution of concentration at time zero and ξ is the space variable.

If the initial concentration distribution is a rectangle between -a and a, then equation (5) reduced to:

$$\frac{c(x,t)}{c_o} = \frac{1}{2\sqrt{\pi t}} \int_{-a}^{a} \exp(-(x-\xi)^2/4t)\, d\xi \qquad (6)$$

where c_o is the initial concentration in the interval between -a and a.

Equation (4) may be solved numerically, using the following explicit equation for marching ahead in time:

$$U_{i,j+1} = rU_{i-1,j} + (1-2r)\, U_{i,j} + rU_{i+1,j} \qquad (7$$

In the above, U is the finite difference approximation for concentration, the i index refers to space, and the j index to time.

The quantity, $r \equiv \frac{\Delta t}{(\Delta x)^2}$ must be less than 0.5 in order to avoid numerical instability (Ames, 1969).

The stability limitation can be avoided using implicit techniques, but such approaches are complicated and not easily modified. Furthermore, the stability limitation is not too serious.

Let us take r = 0.4, and a diffusion coefficient, D, of 100 m^2/second.

$$\Delta t' = \frac{1}{D} \Delta t = r \frac{(\Delta x)^2}{D} \tag{8}$$

Then, the permitted time step varies with spatial grid size as follows:

Δx	$\Delta t'$ (sec)
1 meter	4×10^{-3}
10 m	0.4
100 m	40
1 km	1 hour

It is readily seen from Eq. 8 that, as the diffusion coefficient decreases the maximum time steps become larger.

The diffusion equation does not place any limits on minimum allowable time step. Thus, lower $\Delta t'$ values than given in the table may be used if required by chemical kinetics considerations.

An example is presented in Appendix A.

The one dimensional equation (1) can be applied to either horizontal or vertical diffusion. However, it must be pointed out that the formulation given above makes certain assumptions, namely:

1. Eddy diffusion dominates

2. Atmosphere temperature gradients are small compared with concentration gradients

3. The density effect of stratification may be neglected for vertical distances of interest.

Below 90 km eddy diffusion generally dominates over molecular diffusion. For horizontal calculations, the second assumption restricts us to distances small compared with these involved in "weather" phenomena. We know that, at lower altitudes, horizontal temperature gradients tend to be very shallow, and may reasonably assume the same to be true at higher altitudes, even though very little is known about horizontal temperature variations at altitudes above the cloud level. If the temperature gradients are not shallow, then one can expect significant winds. Generally the spatial and temporal history of wind patterns cannot be accurately determined without doing calculations of the type used in numerical weather forecasting. Thus, it would not be realistic to merely add a thermal term to the diffusion equation.

For vertical calculations, we find that the second and third assumptions restrict us to vertical distances of less than a scale height. This restriction is not serious for the early diffusive behavior of a trail, and is well justified by the resulting mathematical simplicity. The complete equation for vertical diffusivity is given by Strobel (1971) and others.

MULTIDIMENSIONAL DIFFUSION

One-dimensional diffusion gives a different time behavior than diffusion in two or three dimensions. This difference is of very great importance when one wishes to estimate residence times or lifetimes of various atmospheric phenomena. A comparison of the analytical formulations of the solution is given below (Sommerfeld, 1949).

The general solution is:

$$u(x_j t) = \int_j f(\xi_j)\ U(x_j t)\ d\ \xi_j \tag{9}$$

for j = 1 the integration is for one space dimension, for j = 2, two dimensions, and for j = 3, three dimensions.

The kernels U for the three situations are:

$$U = (4\pi Dt)^{-\frac{1}{2}} \exp\left\{\frac{-(x-\xi)^2}{4Dt}\right\} \tag{10}$$

$$U = (4\pi Dt)^{-1} \exp\left\{-\frac{(x-\xi)^2+(y-\eta)^2}{4\ Dt}\right\} \tag{11}$$

$$U = (4_{\pi} Dt)^{-3/2} \exp\left\{-\frac{(x-\xi)^2+(y-\eta)^2+(z-\zeta)^2}{4\ Dt}\right\} \tag{12}$$

The above solutions assume that the diffusion coefficients are equal in all directions, an assumptions which is by no means always valid.

For the sake of discussion, let us further simplify the above set of equations by assuming initial conditions to consist of simple "concentration poles" at the origin, and complete symmetry relative to the various coordinates. The pre-exponential factors remain unchanged, but the exponents become, respectively:

$$\frac{-x^2}{4Dt} \tag{10a}$$

$$\frac{-2x^2}{4Dt} \tag{11a}$$

$$\frac{-3x^2}{4Dt} \tag{12a}$$

It is seen that the behavior of the various exponents is basically the same provided that the magnitude of the diffusion coefficient in two dimensions is one half that for one dimension and in three dimensions D is one third that for one dimension. However, the pre-exponential factors show a fundamentally different time dependence, i.e.

$\frac{1}{\sqrt{t}}$ for one dimension

$\frac{1}{t}$ for two dimensions

$\frac{1}{t\sqrt{t}}$ for three dimensions

B

One can obtain drastically different "lifetimes" depending on the number of dimensions considered.

A comparison between one dimensional and radial diffusion is shown in Figure 2 for a diffusion coefficient of 1000 m^2/sec. The initial wake radius is 10 meters. The time required to reduce an initial concentration from 10^{12} to 10^8 molecules/cc is 1.25×10^6 seconds for one dimensional diffusion but only 250 seconds for the radial diffusion case. A comparison is given between values of D differing by a factor of 10 for radial diffusion. The corresponding decay times also differ by this factor. The case where the initial radius is increased to 316 m is also illustrated.

So far we have considered diffusion in a homogeneous medium, where the diffusivity is the same in all directions. The atmosphere, however, is frequently characterized by a situation where diffusivities in the vertical and horizontal directions are significantly different. Depending on altitude and stratification conditions, horizontal and vertical eddy diffusion coefficients can differ by as much as several orders of magnitude. In the 75 km region, it is reasonable to assume that the ratio of horizontal to vertical eddy diffusion coefficients is approximately ten to one.

It thus becomes necessary to solve the diffusion equation for inhomogeneous conditions:

$$\frac{\partial c}{\partial t'} = D_1 \frac{\partial^2 c}{\partial x^2} + D_2 \frac{\partial^2 c}{\partial z^2} \qquad (13)$$

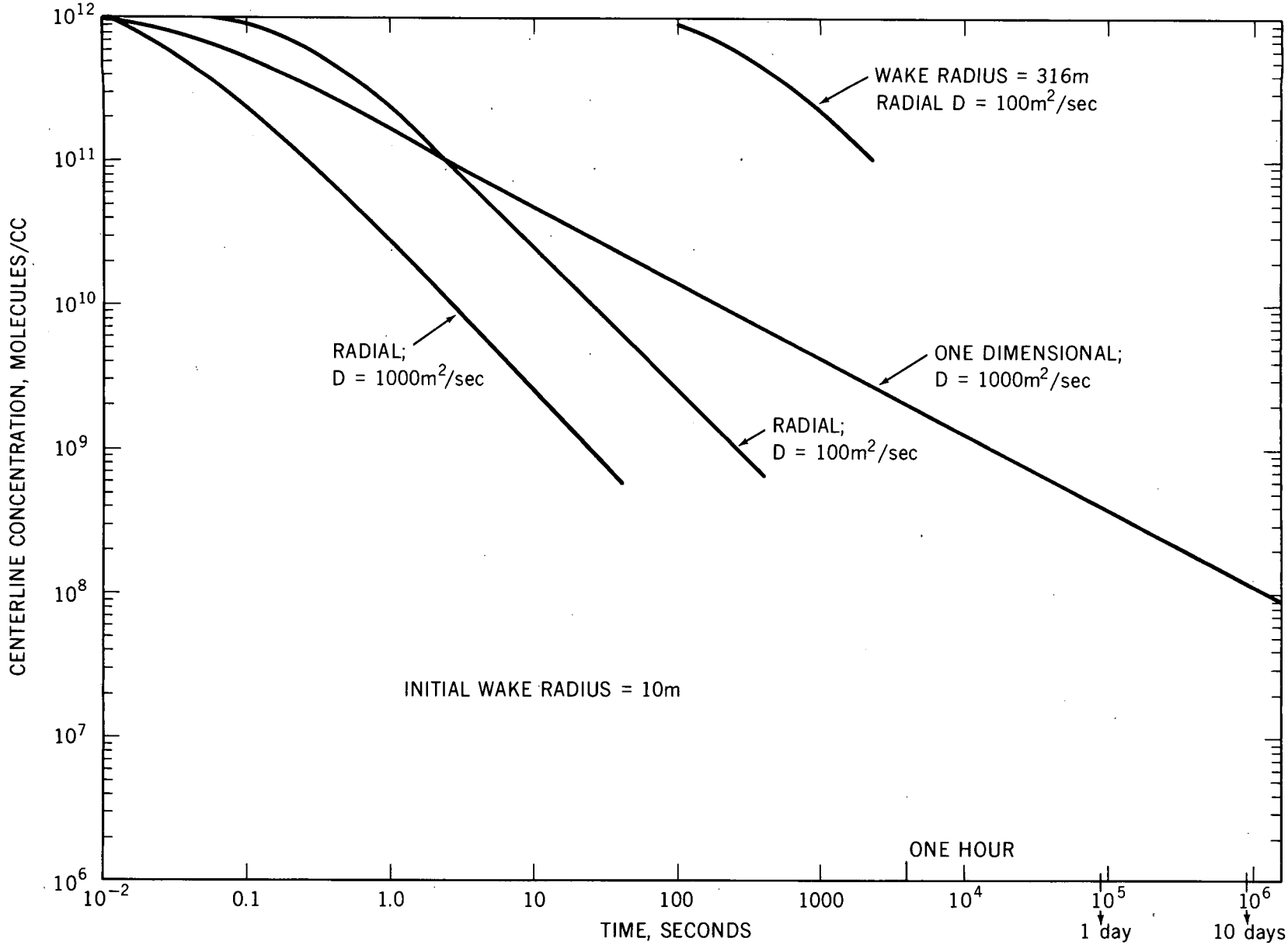

Comparison of one dimensional and radial diffusion

It is, however, possible to examine the behavior of the inhomogeneous system by employing the trick of using different scales in the horizontal and vertical directions. Re-write Eq. 13 in the form:

$$\frac{\partial c}{\partial t'} = D_1 \left[\frac{\partial^2 c}{\partial x^2} + \frac{1}{\beta^2} \frac{\partial^2 c}{\partial z^2} \right] \tag{13a}$$

where

$$\beta^2 \equiv \frac{D_1}{D_2} > 1 \tag{14}$$

Now, define a vertical scale, s, such that

$$s = \beta z \tag{15}$$

Physically, Eq. 15 means that one unit of z corresponds to β units of s. Thus, if $\beta = 100$, then one unit of z, say 1 meter, corresponds to 100 units of s, i.e. 100 cm. Mathematically, we have $s = 100z$, but when dimensions are included, then the expression becomes $s = (100 \text{ cm/m})z$, i.e. the s coordinate corresponds to a finer mesh than the z coordinate.

Equation 13 may be written in dimensionless form as:

$$\frac{\partial c}{\partial t} = \frac{\partial^2 c}{\partial x^2} + \frac{\partial^2 c}{\partial s^2} \tag{16}$$

where $t = Dt'$, and the derivatives are evaluated according to appropriate scales. The formal solution of Eq. 16 is again Eq. 11. However, the differential volume element considered above is a rectangle rather than the usual square.

In finite difference form the two-dimensional diffusion equation becomes

$$U_{i,j,k+1} - U_{i,j,k} = r_x \left[U_{i-1,j,k} + U_{i+1,j,k} - 2U_{i,j,k}\right] + r_y \left[U_{i,j-1,k} + U_{i,j+1,k} - 2U_{i,j,k}\right] \quad (17)$$

where

$$r_x \equiv \frac{D_1 \Delta t}{(\Delta x)^2}$$

$$r_y \equiv \frac{D_2 \Delta t}{(\Delta y)^2}$$

In order to obtain the finite difference form of (16) we need $r_x = r_y$, giving $\frac{D_1}{(\Delta x)^2} = \frac{D_2}{(\Delta y)^2}$; i.e. $\frac{\Delta y}{\Delta x} = \sqrt{\frac{D_2}{D_1}}$.

Again, the direction with the small diffusion coefficient requires a finer mesh.

It appears from the above disucssion that one may examine concentration profiles in both directions, while only using a fine mesh in the direction where diffusion is slow, and gradients steep. If, however, one is not very interested in the detailed development of the vertical profile, then it may be just as well to use equation (17) with $\Delta x = \Delta y$, in which case

$$r_y = \left(\frac{D_2}{D_1}\right) r_x \quad (18)$$

While proper treatment of diffusion in the atmosphere frequently requires use of a two-dimensional calculation,

it is interesting to examine which conditions permit a simplified treatment.

To facilitate visualization of when to make the transition from one-dimensional treatment to two-dimensional treatment, re-write equation (11) in the form:

$$U = AB \tag{19a}$$

where

$$A = (4\pi D_1 t)^{-\frac{1}{2}} \exp\left\{ \frac{-(x-\xi)^2}{4D_1 t} \right\} \tag{19b}$$

$$B = (4\pi D_2 t)^{-\frac{1}{2}} \exp\left\{ \frac{-(y-\eta)^2}{4D_2 t} \right\} \tag{19c}$$

Now $\lim_{D_2 t \to o}(B) = 1$. Thus, in dimensionless form the criterion for using the one-dimensional formulation is:

$$\frac{D_2 t}{(\Delta y)^2} << 1 \tag{20}$$

where Δy is the initial vertical width of the uniform concentration regime.

DIFFUSION WITH CHEMICAL REACTION

One dimensional diffusion with chemical reaction is described by the equation:

$$\frac{\partial c_i}{\partial t'} = D_i \frac{\partial^2 c_i}{\partial x^2} - R_i \tag{21}$$

where R_i is the rate of loss of specie "i".

$$R_i = \sum_{j=1}^{N} k_j c_i c_k \tag{22}$$

R_i is the net loss of specie "i" by the relevant chemical reactions j with species "k"; j and k go from a minimum of one to a maximum of N.

The atmosphere is treated as being isothermal, so that the temperature only comes in at the initial evaluation of the rate coefficient.

One may break up Eq. (21) into two components, i.e.

$$\frac{\partial c_i}{\partial t'} = \frac{\partial c_{iD}}{\partial t'} + \frac{\partial c_{iC}}{\partial t'} \tag{23}$$

where

$$\frac{\partial c_{iD}}{\partial t'} = D_i \frac{\partial^2 c_i}{\partial x^2}$$

and

$$\frac{\partial c_{iC}}{\partial t'} = -\sum_{j=1}^{N} k_j \, c_i \, c_b$$

The space field can be swept for chemical reaction during a time step, Δt, followed by a sweep for diffusive relaxation for that same time step. In this way it is possible to use the explicit marching formula for diffusive relaxation, and Runge-Kutta for the solution of a set of coupled nonlinear first order equations.

To check the validity of the above procedure a comparison was run between the method described above, and a direct solution of Eq. (21) as written. No difference could be seen in the results. The Euler method was used for the chemical component in both cases.

Computations were carried out for one dimensional diffusion with kinetics, radial diffusion with kinetics, and two dimensional diffusion with kinetics. The rationale behind the computational methods has already been discussed and will not be repeated here. Solutions to the two dimensional diffusion equation with chemistry are presented for illustrative purposes both as three dimensional plots, and as contour plots. In both situations a series of "frames" developed in time are shown. Figure 3 shows a three dimensional projection of the three chemical species. The horizontal diffusion coefficient is 10^4 cm^2/sec, and the vertical coefficient is 10^3 cm^2/sec. Figure 4 shows contour plots for a similar situation.

APPLICATION TO THE SPACE SHUTTLE

A space shuttle reentry schematic is shown in Figure 5. Three basic regimes may be distinguished. First is the "near" wake mixing regime where eddy diffusivity is determined by turbulence generated by shear due to the high reentry velocity. This regime has been treated by Park (1972) who used a model developed by Lin and Hays (1965). The Lin-Hays model is quasi-one dimensional, and primarily designed as a method to treat wake chemistry without regard to radial wake gradients which are assumed to be zero.

In using this model Park assumes that the initial wake radius for the shuttle is 7.6 m and that its boundary varies according to the formula

TIME = 1000 SEC
ΔX = 10 METERS

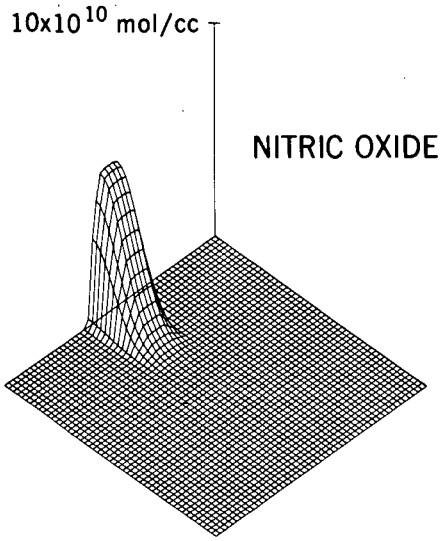

TIME = 20,000 SEC
ΔX = 10 METERS

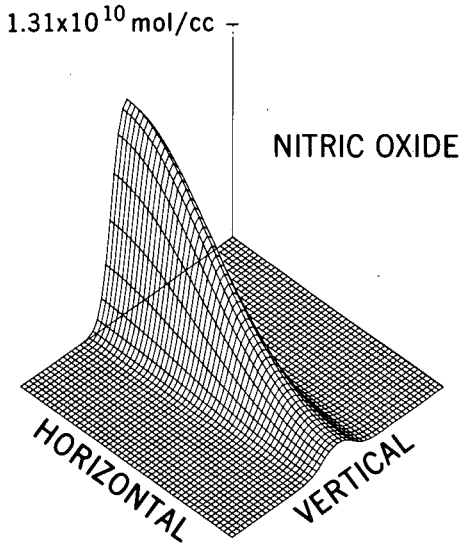

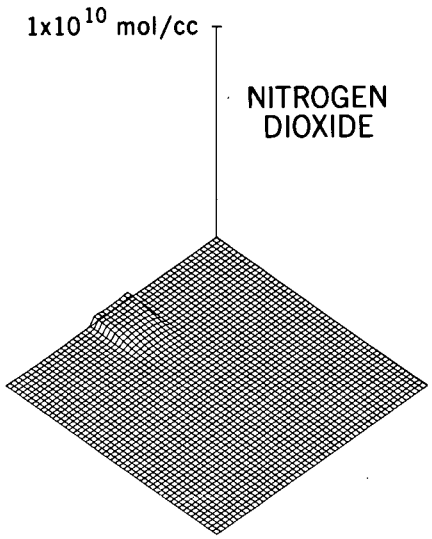

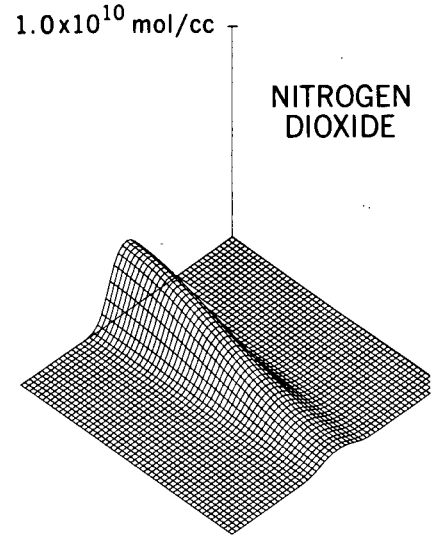

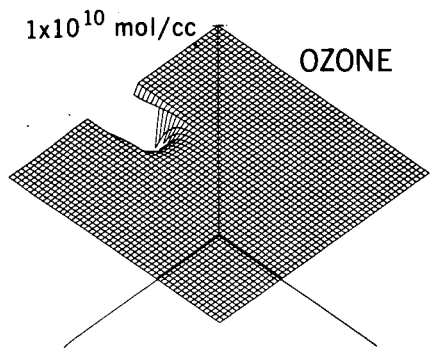

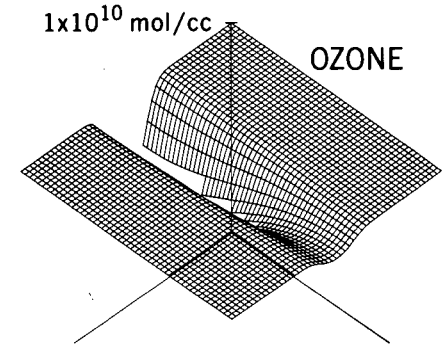

CONTOUR PLOTS

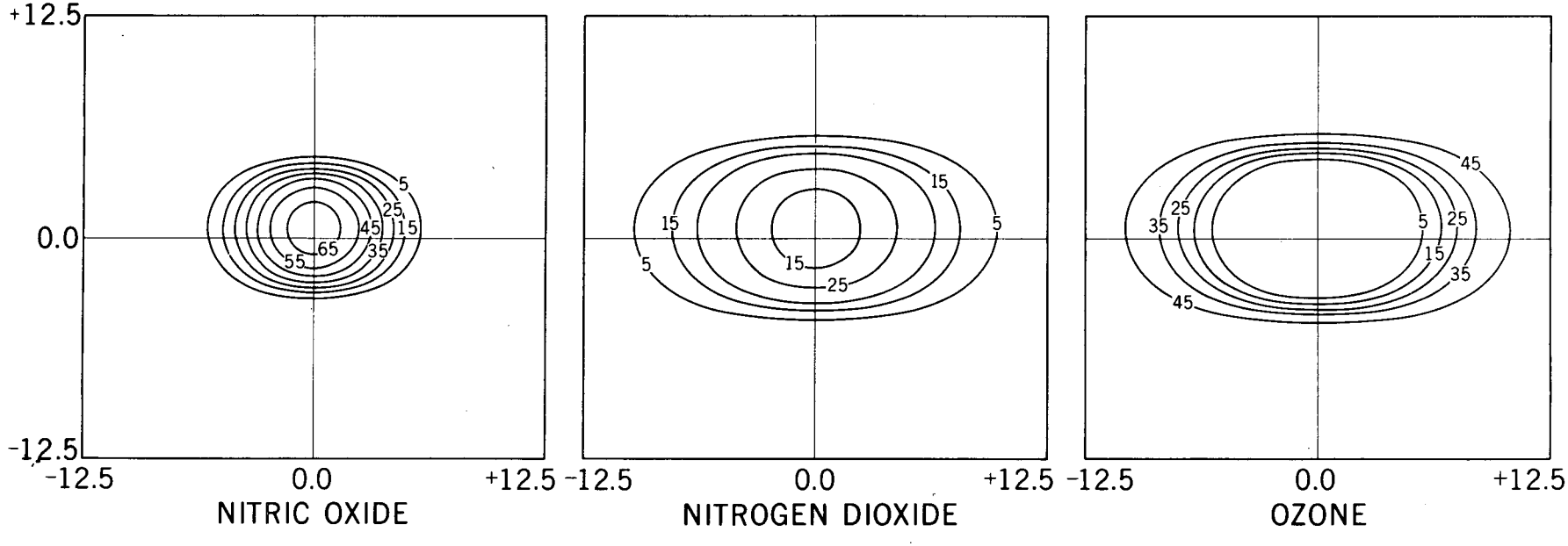

WAKE MIXING
30 KM
5 SEC
$10^{14} \rightarrow 10^{12}$ (NO)
ATMOSPHERIC MIXING
$10^{12} \rightarrow 10^{9}$ (NO)
1 DAY - 10 DAYS
ATMOSPHERIC CHEMISTRY
10^{9} - BACKGROUND
AFTER ONE DAY

$$\frac{r_b}{r_o} = 0.7 \left(\frac{s'}{r_o}\right)^{1/3} \tag{24}$$

where r_b is the wake radius at any point, r_o the initial wake radius and

$$s' = s_o' + x \tag{25}$$

is the distance from a hypothetical apex of the wake. x is the distance from the section where $r_b = r_o$. s_o' is the distance from the hypothetical apex to the section where $r_b = r_o$. For $r_o = 7.6$ meters, $s_o' = 21.6$ meters. Also, define a quantity L' as the distance from the leading edge of the vehicle to the section where $r_b = r_o$. Reference to Figure 9 in Park (1972), reproduced in the Appendix as Figure A-4, shows that L' is approximately 91.5 meters. Park also defines a quantity, s as the distance from the leading edge of the vehicle. We have

$$s \equiv L' + x \tag{26}$$

Consider a wake radius, r_b of 23 meters, giving $\frac{r_b}{r_o} = 3$. Calculating back from Eq. 24 one obtains $s' = 600$ meters. From Equations 25 and 26 we then deduce that s, the distance from the leading edge, is 670 meters (2200 ft.).

Reference to Park's Figure 10, which shows the amount of air converted to nitric oxide as a function of distance from the leading edge of the vehicle at 70 km indicates that 670 meters is the section at which the ratio of nitric

oxide mass produces to mass of air swept is at a maximum. The ratio varies between approximately 2.5% and 9% depending on vehicle entry velocity. The mole fraction variation is approximately the same. According to Goldburg (1965) 610 m is approximately the point where transition from a laminar to a turbulent wake occurs. Thus, 670 m is some 60 m into the turbulent wake regime. The $\frac{x}{D}$ value at 670 m is 38, where $D \equiv 2\ r_b$.

Reference to Bailey (1966), Li (1963) and Slattery and Clay (1962) shows that at the section considered above, the wake centerline velocity is still some 10% of vehicle velocity, i.e. in the order of 610 m/sec.

However, the wake centerline velocity is down to 1% of vehicle velocity, i.e. 61 m/sec at $\frac{x}{D} = 420$. Such a value is comparable to wind speeds at 75 km altitude (Smith et al., 1964). The above value corresponds to $s = 7{,}400$ m giving $r_b = 52$ meters. At $s = 3 \times 10^4$ m the wake velocity would decrease to 9.1 m/sec (Park, 1972) which is the same order as the velocity of natural turbulence. At this point the wake radius, r_b, would be 132 meters.

In the "near" wake mixing situation discussed above eddy diffusivity is determined by turbulence generated by shear due to the high reentry velocity. This regime may be treated using a time dependent eddy diffusivity whose form can be deduced by matching to the empirical wake growth law or in the manner of Park (1972). The use of a time

dependent eddy diffusivity combined with chemistry is actually superior, as it takes account of radial gradients existing in the wake. These gradients are assumed to be zero in the Lin and Hayes (1965) model used by Park. The time dependent eddy diffusivity approach is an interesting possibility for future study.

For the present we have assumed that the Park-Teare calculation is valid up to a certain point in the wake, after which the dominant process becomes atmospheric mixing with constant eddy diffusivity. The proper point of transition from wake generated turbulence to atmospheric turbulence is not constant, but depends very much upon atmospheric conditions. The more turbulent the atmosphere, the sooner atmospheric mixing becomes dominant, and vice versa.

Referring once again to Figure 5 the second basic regime may be termed the atmospheric mixing regime. Chemical reactions are important, but affect eddy diffusive processes primarilty through modification of the boundary conditions for the diffusive process.

In the third regime, concentration gradients have become very shallow, and the rate of diffusion slow. Chemical rate processes now play the dominant role. This regime provides proper input parameters for more sophisticated chemical reaction models of the atmosphere.

Figure 6 shows the centerline nitric oxide concentration for a reentering shuttle. Initial conditions for the

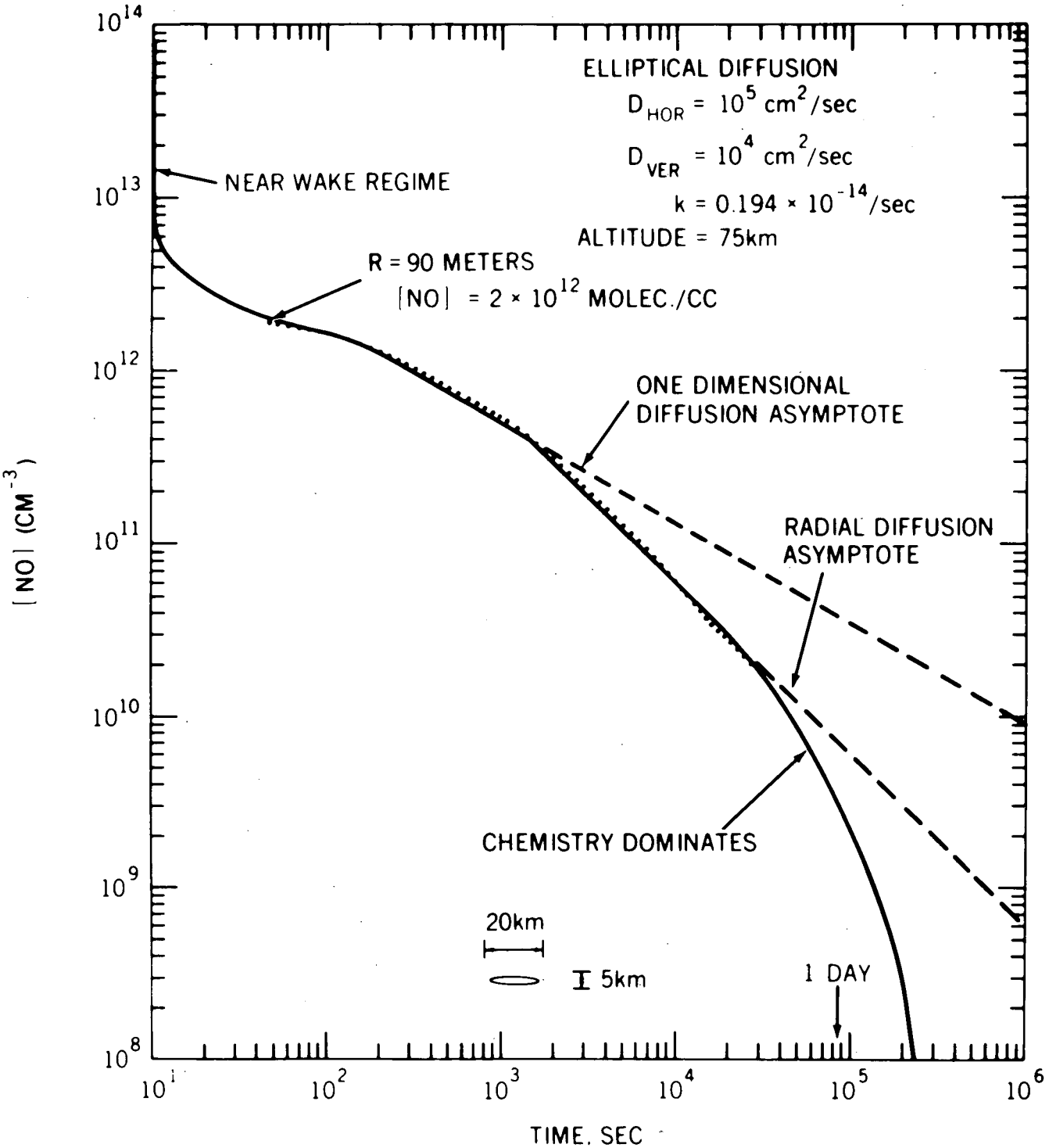
ELLIPTICAL DIFFUSION
$D_{HOR} = 10^5$ cm^2/sec
$D_{VER} = 10^4$ cm^2/sec
$k = 0.194 \times 10^{-14}$/sec
ALTITUDE = 75km
NEAR WAKE REGIME
R = 90 METERS
[NO] = 2×10^{12} MOLEC./CC
ONE DIMENSIONAL DIFFUSION ASYMPTOTE
RADIAL DIFFUSION ASYMPTOTE
CHEMISTRY DOMINATES
20km
5km
1 DAY
[NO] (CM^{-3})
TIME, SEC
10^{14}
10^{13}
10^{12}
10^{11}
10^{10}
10^{9}
10^{8}
10^{1}
10^{2}
10^{3}
10^{4}
10^{5}
10^{6}

atmospheric calculation were taken as follows: nitic oxide concentration is taken as 200 x 10^{10} molecules/cc, and initial radius as 90 meters. The ratio of horizontal to vertical eddy diffusivity is taken to be ten, the diffusivity coefficients being 10^5 cm^2sec^{-1} (10 m^2/sec) horizontal and $10^4 cm^2 sec^{-1}$ (1.0 m^2/sec) vertical. These are conservative estimates, and cases with other values of eddy diffusivity will be discussed later. Extrapolations for one dimensional and radial diffusion are shown, and transition to the chemically dominant regime is seen to occur after approximately one day. Figure 7 shows development of concentration profiles with time in both the vertical and horizontal directions. In this case we started with a situation where initial ozone concentration grows monotonically with time. A more interesting quantity in this case is the "ozone hole". Figure 8 shows development of the half width of the point of 50% ozone depletion, i.e. inside the radius shown ozone concentration is less than 50% of the natural ambient value. For the case considered in Figures 6 and 7 we see in Figure 8 that the maximum horizontal spread of the ozone hole occurs in approximately 3 hours, and amounts to a 400 meter half width for the 50% point. After approximately 5 hours, the gap begins to close, and after 10 hours the 50% point has moved to the center of the trail. At 20 hours, centerline ozone concentration is 85% of the ambient value, whereas centerline nitric oxide concentration is still 20 times as

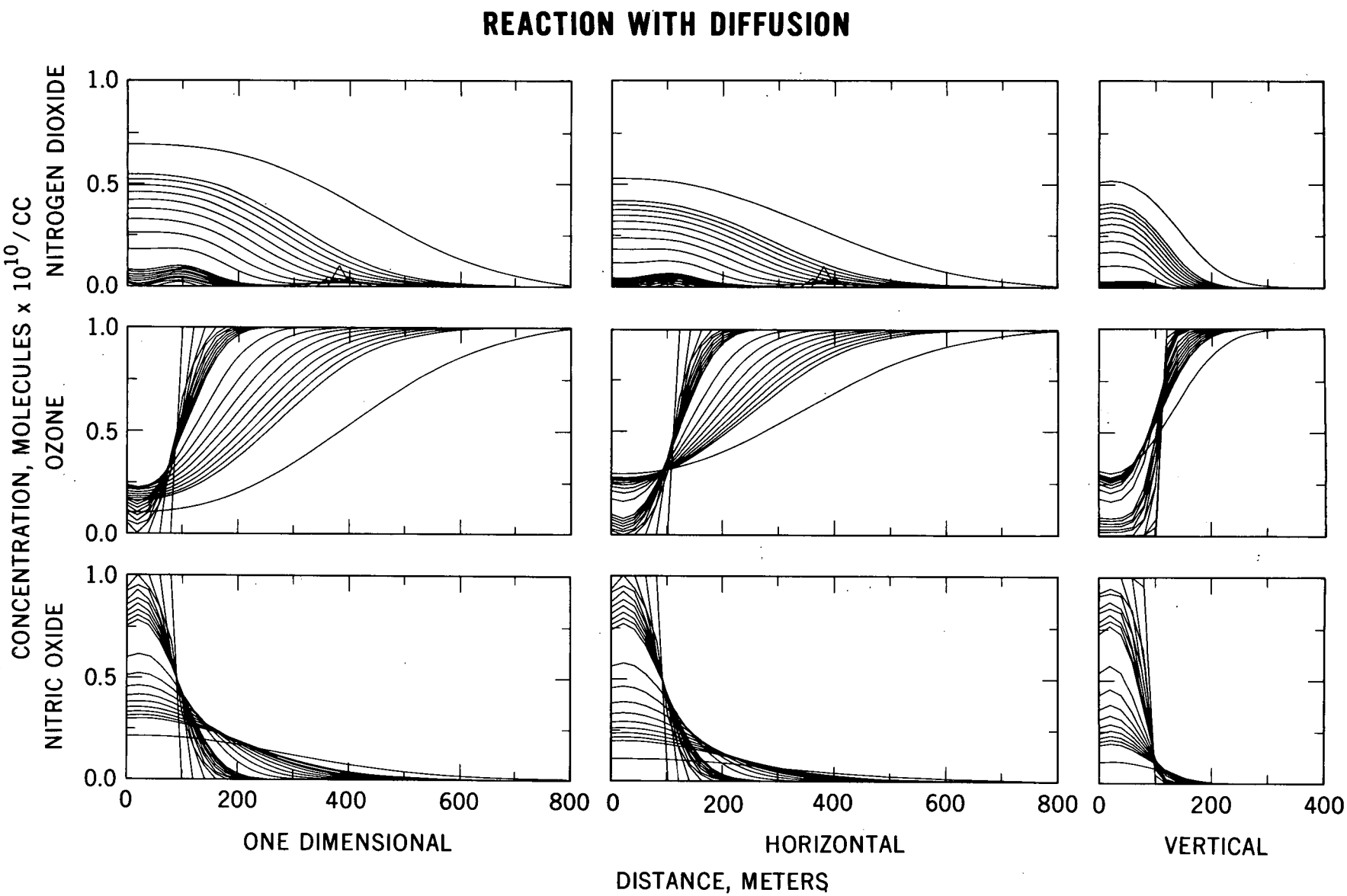
REACTION WITH DIFFUSION
CONCENTRATION, MOLECULES x 10^{10} / CC
NITROGEN DIOXIDE
OZONE
NITRIC OXIDE
1.0
0.5
0.0
0
200
400
600
800
ONE DIMENSIONAL
HORIZONTAL
VERTICAL
DISTANCE, METERS

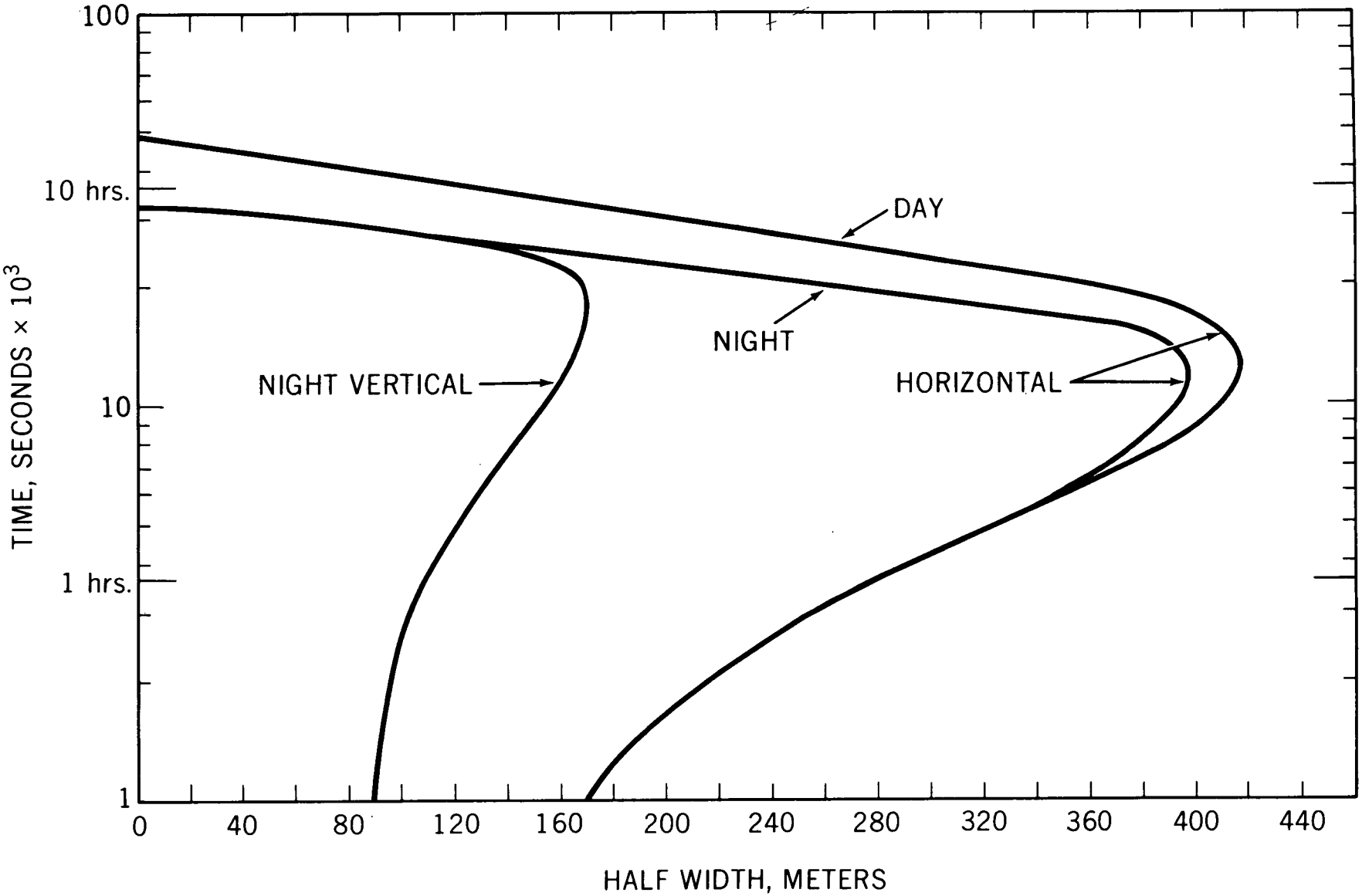

Time dependence of half width of 50% ozone depletion

high as the natural background. The vertical extent of the ozone depletion is less, since the vertical diffusion coefficient has been taken to be only 10% of the horizontal value. Otherwise, vertical behavior is quite similar to horizontal behavior.

Thus far, we have only discussed what may be considered a "night time" situation, i.e. nitric oxide reacts with ozone to give nitrogen dioxide whose further chemical activity is not considered. However, much of the alarm about nitric oxide pollution has referred to the "daytime" situation in which nitrogen dioxide is photodissociated to nitric oxide, thus creating a catalytic cycle in which ozone is destroyed without any corresponding reduction in odd nitrogen. The purely photochemical case is serious indeed. However, Figure 8 shows that in the diffusive situation the recycling of nitric oxide has a relatively minor effect. The peak half width of the ozone hole is increased by only 5%, while the collapse time goes from 32,000 seconds to 48,000 seconds, i.e. from 9 hours to 13 hours. Figure 9 shows nitric oxide decay for both night and day situations. The daytime nitric oxide does decay more slowly as expected, but the difference between daytime and nighttime cases only becomes significant for long times. It might be noted that, for the daytime situation, nitric oxide concentration is govered only by diffusion, since any nitric oxide which reacts with ozone is almost immediately recycled because of the rapid

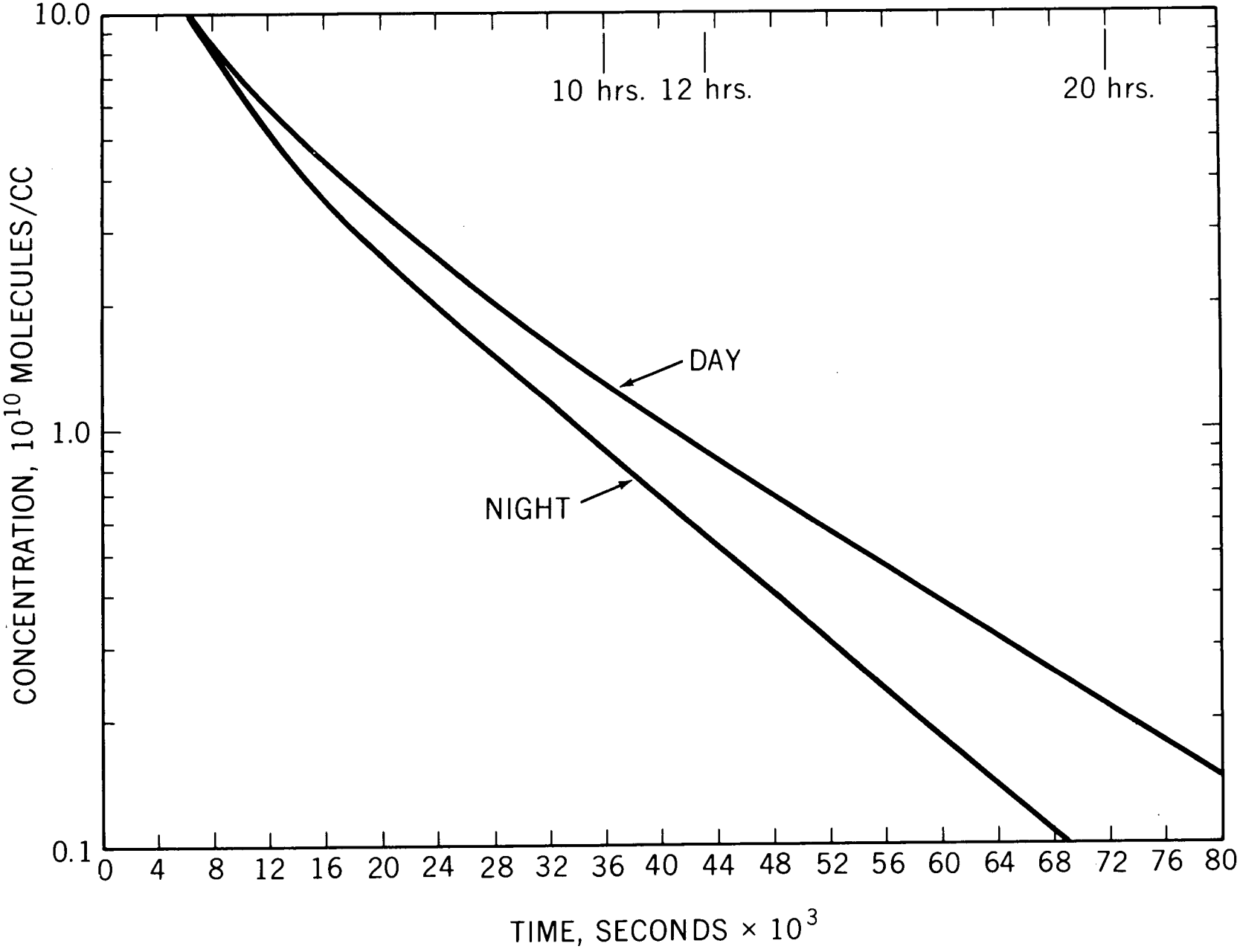

Centerline nitric oxide decay

photodissociation rate. In the situation considered, it was assumed that ozone concentration is zero in the space originally occupied by the nitric oxide. Thus, ozone concentration increases monotonically to some asymptotic value. At the other limit, where background ozone concentration extends into the core of the initial high nitric oxide concentration regime, a rapid chemical reaction occurs, bringing ozone in the core region to a very low concentration, i.e. a situation very similar to the one considered. We see from Figure 10 that the initial increase in centerline ozone concentration is very rapid, a behavior attributable to initially steep concentration gradients and small effect of chemistry. In half an hour a plateau region is reached which lasts for approximately four hours. The plateau is the regime of most active chemical reaction, as is also evident from the nitrogen dioxide plot which reaches a maximum in this time period. A look at the rate constant for the reaction:

$$NO + O_3 \rightarrow NO_2 + O_2$$

explains the behavior obtained. The rate constant for the above reaction is 0.2×10^{-4} seconds when concentrations are measured in terms of 10^{10} molecules per cubic centimeter. When the plateau is reached, the ozone concentration is 0.3 in the above units, while nitric oxide concentration is 10. Thus, for the above chemical reaction:

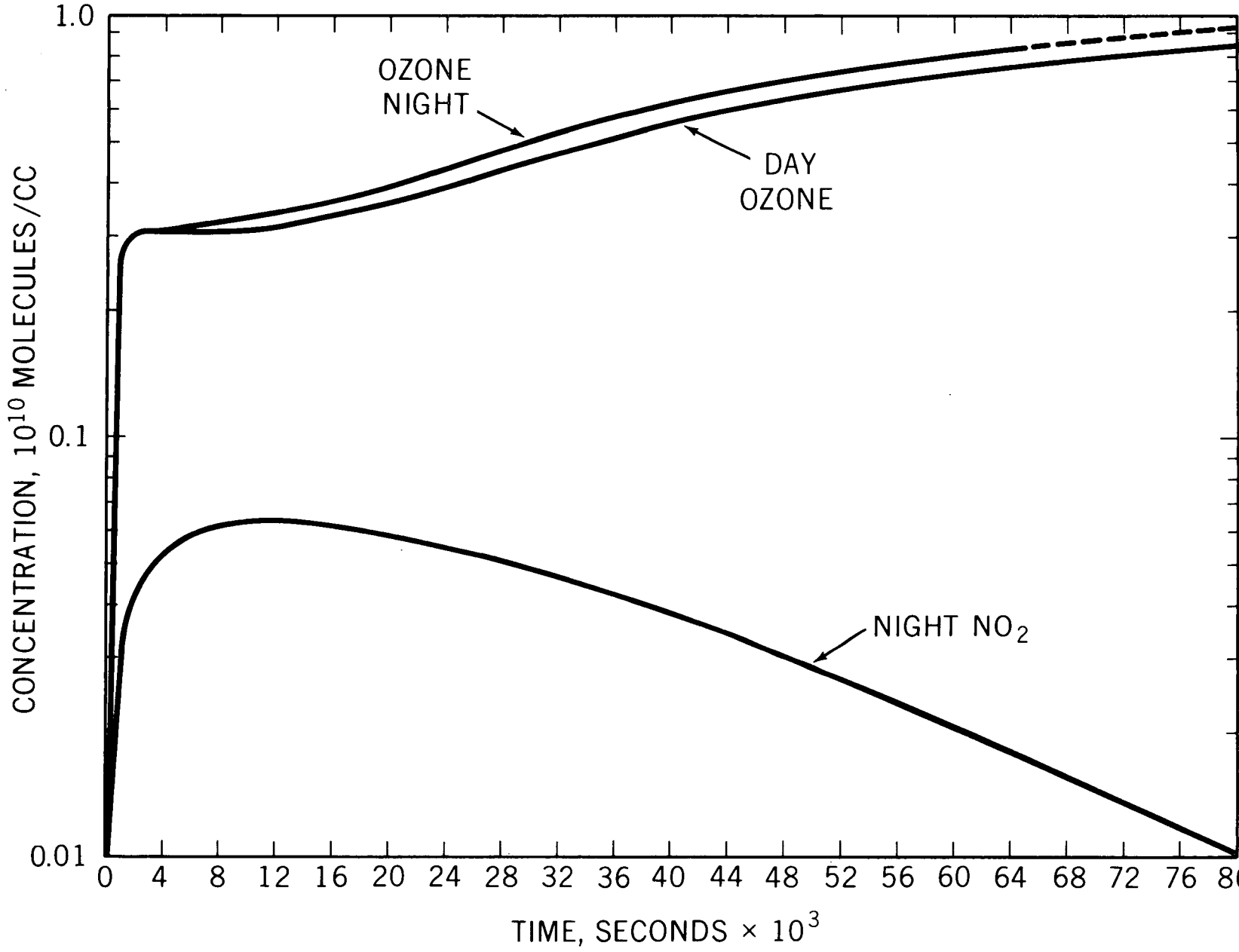

Ozone recovery (centerline)

$$\frac{d}{dt}[NO_2] = (0.2\times10^{-4}sec^{-1})(10)(0.3) = 0.6\times10^{-4}sec^{-1}$$

giving a characteristic time of approximately 2×10^4 seconds, which is indeed seen to be characteristic for the nitrogen dioxide buildup. As the ozone buildup leaves the plateau region at 16×10^4 seconds, the nitric oxide concentration has already decreased to 4.5, and at 34×10^4 seconds the nitric oxide concentration is down by a factor of ten to 1.0, while ozone has only increased by a factor of two, thus decreasing the nitrogen dioxide production rate to $0.1\times10^{-4}sec^{-1}$. However, the rate of outward diffusion has only increased, since centerline nitrogen dioxide concentration is greater than before. Thus, the nitrogen dioxide concentration begins to drop, and continues to do so, since the rate of production continues to decrease.

Reference to Figure 10 shows that nitrogen dioxide concentration is always below 0.7×10^{10} molecules/cc. Thus, one would expect the photodissociation back to nitric oxide to become important only after nitric oxide concentration becomes comparable. References to Figure 8, 9 and 10 however, indicate noticeable difference between night and day situations as early as 6×10^4 seconds, which is the point at which maximum nitrogen dioxide concentration is approached. Furthermore, it is found that the daytime nitric oxide concentration is the sum of nighttime nitric oxide and nitrogen dioxide, at least for time in excess of half an hour. A

steady state analysis of the daytime chemistry shows that nitrogen dioxide concentration is approximately 0.2% of the nitric oxide value. This is quite different from the nighttime situation where nitrogen dioxide concentration actually exceeds nitric oxide concentration for times longer than 15 hours.

The cases discussed above all have diffusion coefficients of 10^5 cm^2/sec horizontal, and 10^4 cm^2/sec vertical. These estimates are conservative, representing reasonable lower limits to diffusion coefficients which may be expected at 75 km altitude. However, it is essential to recognize that knowledge of atmospheric diffusion coefficients is very sparse, and that large variations in eddy diffusivity are quite probable.

For the daytime situation, where the effect of chemistry on nitric oxide concentration is slight, one may expect that the time required to reach background concentration levels is inversely proportional to the diffusion coefficient. One obtains approximately the same behavior for nighttime centerline nitric oxide concentration, although the proportionality is no longer quite accurate. For centerline ozone concentration such simple proportionality generally does not hold, and a more complete analysis is needed.

To study the effect of eddy diffusivity, we ran three cases in which the initial conditions were identical, the number of time steps were the same, but the eddy diffusion

coefficients were varied. The situation of homogeneous radial diffusion was chosen for this comparison. The initial radius was taken to be 20 meters, and the initial nitric oxide concentration was 10^{14} molecules/cc. Results of the above comparison are given in the following table:

$D, m^2/sec$	t'(sec)	Dt'/r_o^2	[NO]	$[O_3]$
100	$2x10^3$	500	$6x10^{10}$	$0.8x10^{10}$
10	$2x10^4$	500	$5x10^{10}$	$0.21x10^{10}$
1.0	$2x10^5$	500	$5x10^{10}$	$0.2x10^8$

where r_o is initial radius and t' is time after 20,000 intervals. It is seen that for constant values of the quantity (Dt'/r_o^2) the centerline nitric oxide concentration is approximately the same, but that centerline ozone concentration decreases for decreasing diffusion coefficient. The reason for the above behavior is that the slower the diffusion, the longer the chemical destruction of ozone can proceed before nitric oxide concentration drops to a low value. A comparison of concentration-time histories is shown in Figure 11. The eddy diffusion coefficient is varied.

Figure 12 shows a comparison of one dimensional two dimensional, and radial diffusive behavior. The one dimensional centerline concentration decay approaches a $t^{-\frac{1}{2}}$ asymptote, and the radial decay has a t^{-1} asymptote. For

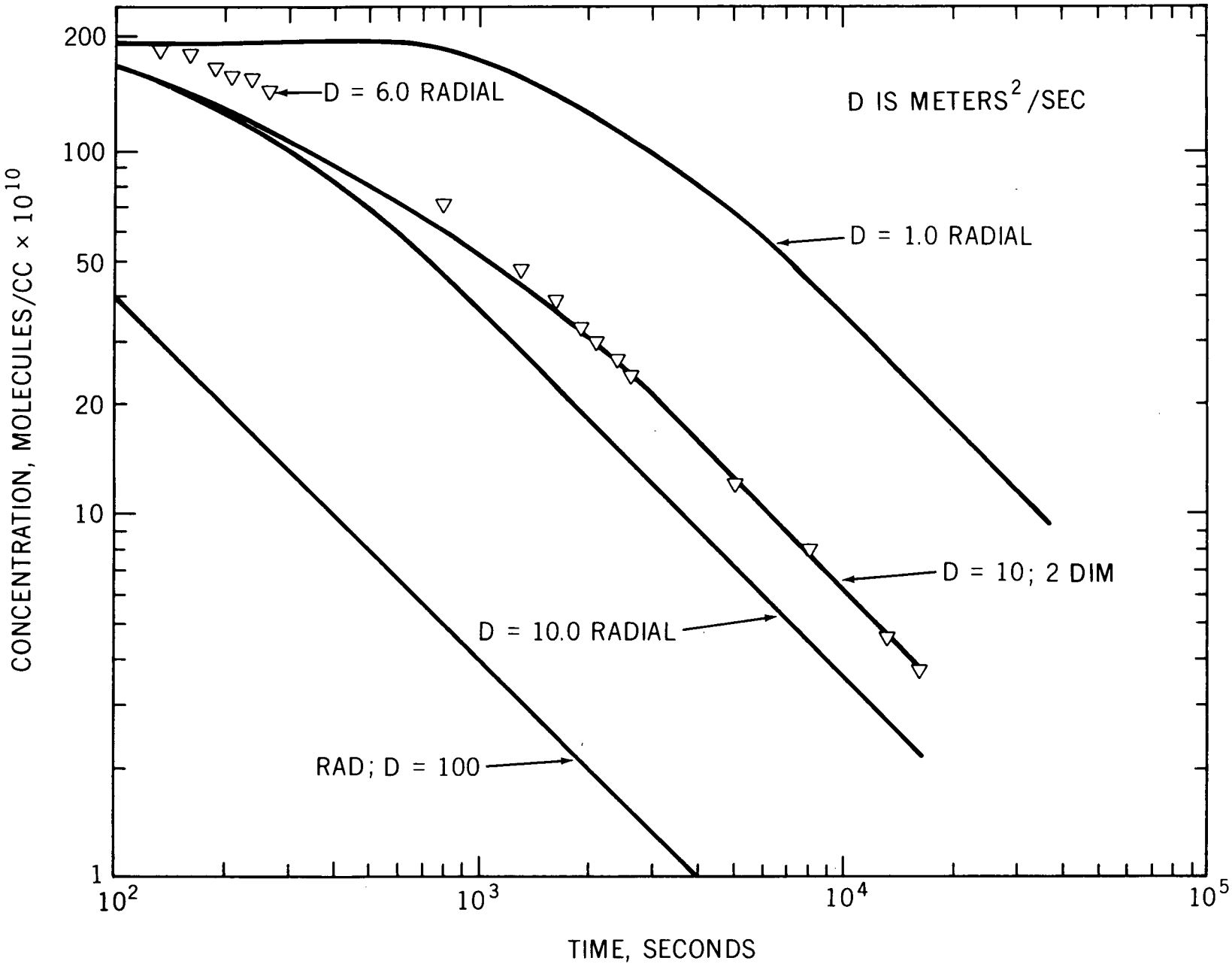

Dependence of centerline concentration on diffusivity

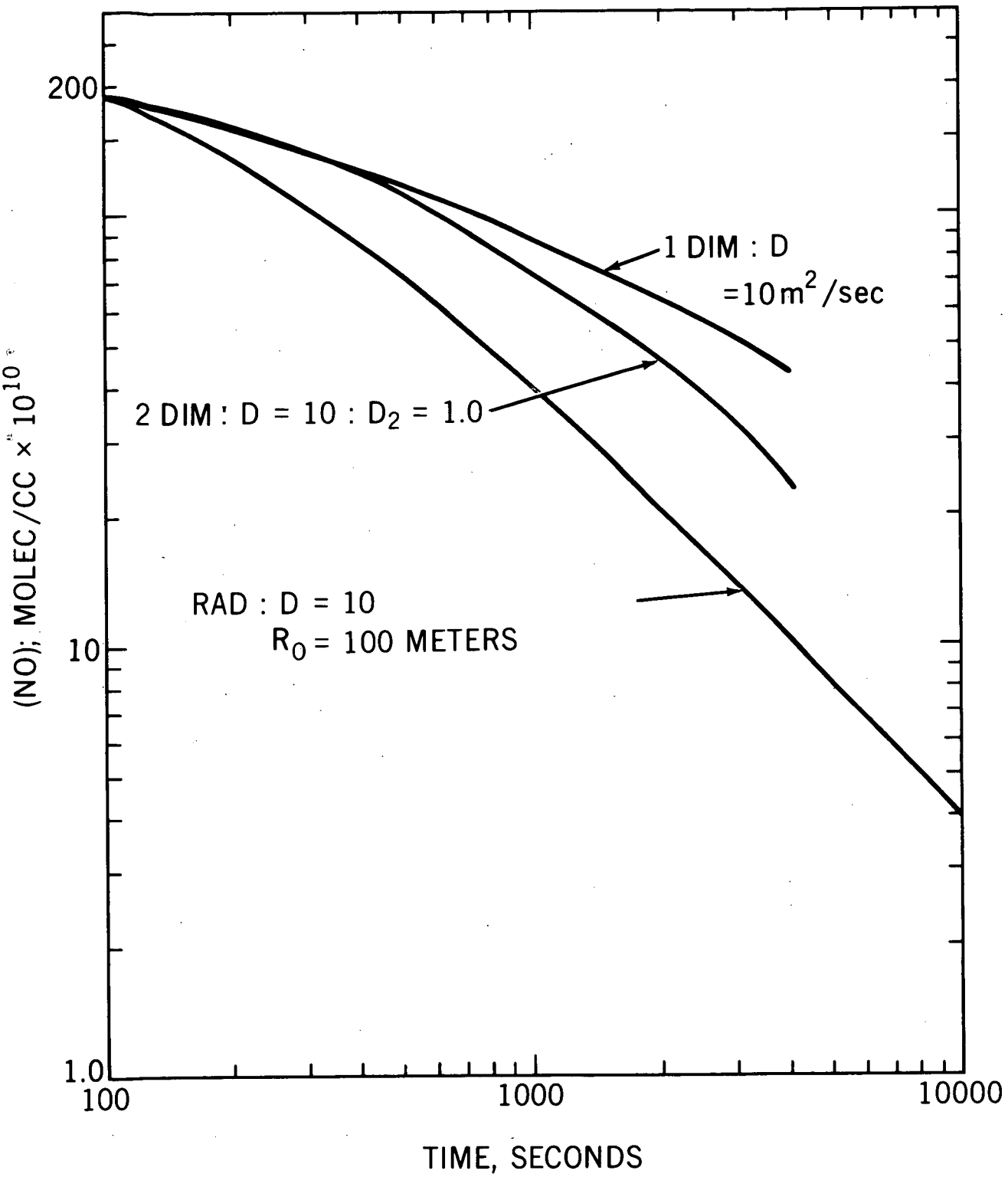

Comparison of one-dimensional, two-dimensional and radial diffusion

the two dimensional case, we took the ratio of vertical to horizontal eddy diffusivity to be 0.1. The graphs on Figure 12 show that the two dimensional case is initially close to one dimensional behavior, then approaches a radial type time decay for long times. Reference to equations 19 and 20 shows that the above behavior is precisely what one would expect from theory. There, it was found that one dimensional behavior would be observed when:

$$\rho = \frac{4D_2 t'}{r_o^2} \ll 1$$

where D_2 is vertical eddy diffusion coefficient. From Figure 12 we see that at $t' = 1{,}000$ seconds deviation from one dimensional behavior is 17% and at that point the quantity ρ is equal to 0.4. A more general examination of the differences between the two curves shows that, very roughly, the deviation from one dimensional behavior is equal to (ρ/π). Radial time decay is reached when $\rho > 1$. However, the effective diffusion coefficient is some mean of vertical and horizontal coefficients. For the particular case chosen above, the best mean is simply the arithmetic average of the coefficients in the two directions, but such simplicity is seen to be fortuitous when other ratios of vertical to horizontal diffusivity are considered.

THE EFFECTS OF WINDS

Thus far, winds have been considered implicitly, as generators of the background turbulence which gives rise

to the eddy diffusivity. Winds also affect the persistent wake in two other ways, namely advection and distortion. The former is, of course, due to a steadily blowing wind, while the latter is caused by wind shear.

First, consider the effect of advection. Berman and Goldburg (1971) quoted an annual mean zonal wind velocity of 10 meters/second for the stratosphere. The work of Smith et. al., (1966) suggests higher wind speeds at higher altitudes. Taking 10 m/sec as a reasonable lower limit, one finds that in 10,000 seconds (approximately 3 hours) a North-South trail will have been wafted some 100 km in the direction of the prevailing wind. A trail originally deposited in the East-West direction will have been moved along its own axis, giving little indication of wind effect. The above argument assumes a purely zonal wind, while a wind having both zonal and meridional components is probable more realistic. In that case, the corresponding effects are determined by the proper components of the wind vector relative to the wake axis.

Extrapolation of higher altitude wind shear data of Bedinger and Constantinides (1969) to 75 km indicates an average vertical shear of 7 meters/second/kilometer, or 0.7 meters/second/100 meters. Thus, two horizontal layers, separated in altitude by 100 meters, would move at an average rate of 0.7 meters/second relative to each other. In three hours, the displacement would therefore be as large as 7 km.

If the wind shear is perpendicular to the trail axis, then the trail cross section will be stretched out into a thin oval shape, decreasing the thickness of the ozone hole, and increasing the rate of dissipation of nitric oxide. On the other hand, a trail whose axis is parallel to the axis of shear will only suffer a slight distortion in the vertical concentration profile.

Figure 13 shows the effect of wind shear perpendicular to the wake axis. Compare Figure 13 with the vertical section of Figure 7. Note that the effect of shear is to slant the concentration profiles as gas from the periphery is moved closer to the center. Figure 14 gives a comparison of centerline nitric oxide concentration with, and without wind shear. Nighttime chemical conditions were chosen. It is readily seen that wind shear plays quite an important role, and should be studied in greater detail.

EFFECT OF THE BOW SHOCK

Park (1972) considered the nitric oxide produced in the stream tube which becomes the wake of the vehicle, and the present report has been concerned with the transient effect of the wake nitric oxide. However, there is additional nitric oxide produced by the extended bow shock. To properly estimate the amount thus produced one needs to know the exact shape of the bow shock, as well as the flow characteristics in the stream tubes behind it. The above requires a detailed aerodynamic calculation not available

EFFECT OF SHEAR
CONCENTRATION, MOLECULES x 10^{10}/CC
NITRIC OXIDE
OZONE
NITROGEN DIOXIDE
VERTICAL DISTANCE, METERS
0
0.2
0.4
0.6
0.8
1.0
80
160
240

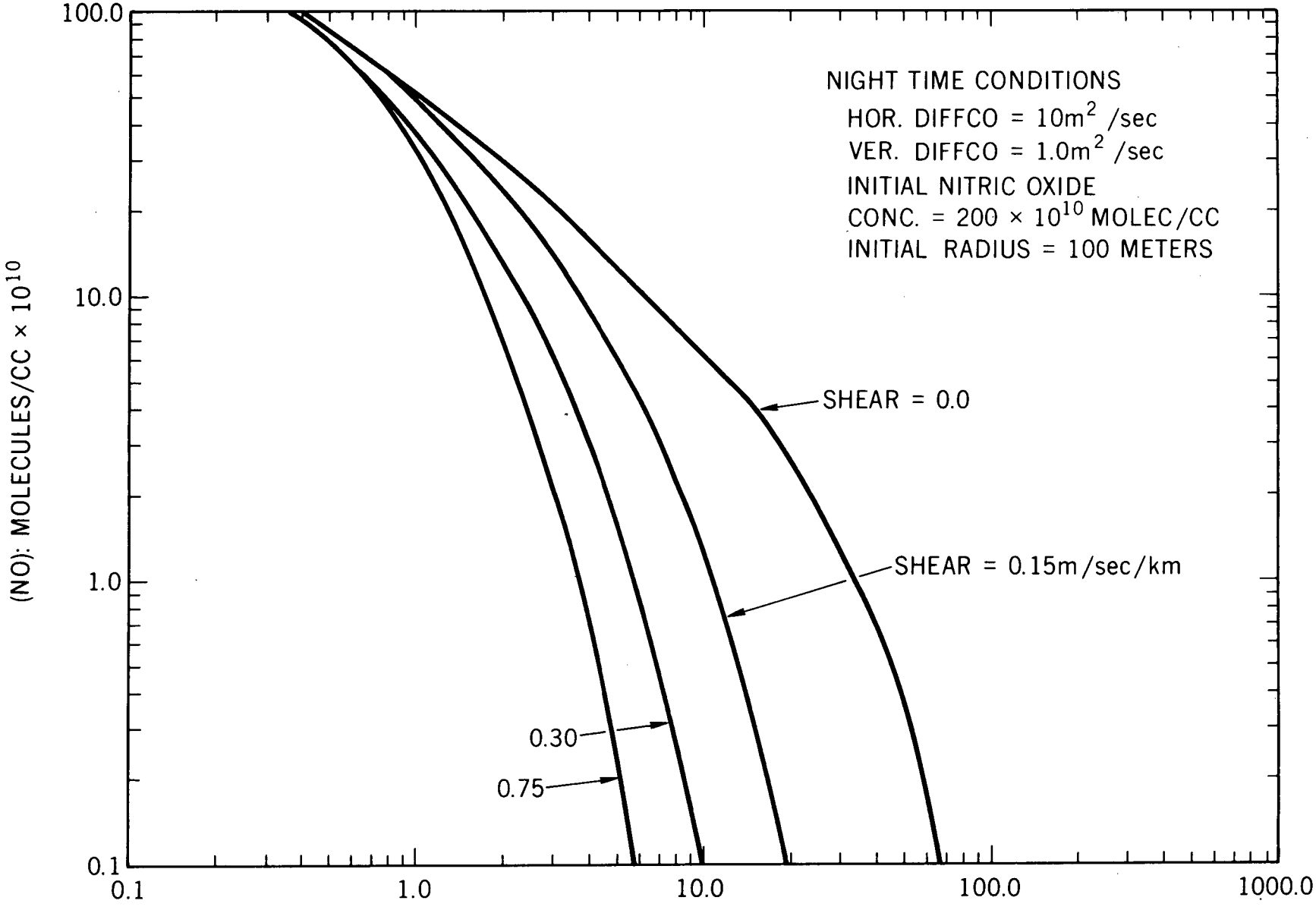

Effect of vertical shear

to the author. For a rough estimate it was assumed that the bow shock produces a nitric oxide concentration of 10^{13} molecules/cc (i.e. 1%) over an initial radius of 400 meters.

The horizontal diffusivity was taken to be 100 m^2/sec, and the vertical diffusivity was 10 m^2/sec. It was found, that in the absence of shear the ozone hole after 12 hours is some 3.5 km wide, and centerline ozone concentration is 0.3% of background. However, introducing a perpendicular shear of 1.25 m/sec/km made the ozone hole close after 4 1/2 shours.

The above calculation is only a rough estimate, but it shows the importance of a detailed calculation of the bow shock production of nitric oxide.

ENHANCEMENT OF THE LOWER IONOSPHERE BY NITRIC OXIDE INJECTION

The nitric oxide and nitrogen dioxide resulting from the reentering body, can be ionized by direct solar Lyman alpha radiation during the day and by scattered Lyman alpha radiation at night. A starting NO density of 10^{12} cm^{-3} at 75 km will give rise to 2×10^6 electrons/cm^3 for a zenith angle of 7.5^o. This is more than three orders of magnitude above the normal background. The majority of the primary NO^+ and NO_2^+ ions formed dissociatively recombine with free electrons. However, ionic reactions do occur which modify the primary species. For instance NO_2^+ is transformed into NO^+ by the reactions

$$NO_2^+ + NO \rightarrow NO^+ + NO_2$$

The ion NO^+ can react with NO, CO_2 or N_2 to form a cluster ion which in turn is transferred into a hydrated ion of the form $H_3O^+ \cdot (H_2O)_n$. Such hydrated ions may further cluster to form an aerosol under proper conditions of humidity, pressure and temperature. The dissociative recombination rate of hydrated ions is as much as a factor of 10 larger than that of NO^+ or NO_2^+. In general the electron density is great enough that NO^+ and NO_2^+ will directly recombine but as the electron density decreases the percentage of hydrated ions will increase.

REACTIONS BETWEEN HEAT SHIELD ABLATED MATERIAL AND THE ATMOSPHERE

It is understood that if an ablative heat shield is used one possible product of ablatement is Si. This material can form long-lived ions. These ions normally recombine with electrons by the process of radiative recombination

$$Si^+ + e \rightarrow Si + h\nu$$

and have a rate coefficient of approximately $1 \times 10^{-12} cm^3 sec^{-1}$ which yields a long lifetime. In addition to photoionization Si^+ can be created by charge transfer with other molecular ions by reactions such as

$$NO^+ + Si \rightarrow Si^+ + NO_2$$

and

$$NO_2^+ + Si \rightarrow Si^+ + NO_2$$

Molecular ions involving Si can be formed by association

$$Si^+ + XO \rightarrow SiO^+ + X$$

where XO is a neutral such as O_2. The ion SiO^+ would then recombine at a rate of the order of 4×10^{-7} cm^3 sec^{-1}, which is orders of magnitude faster than radiative recombination. However, the reaction

$$SiO^+ + O \rightarrow Si^+ + O_2 + 0.6 \text{ ev}$$

also occurs with a rate coefficient of 2×10^{-10} cm^3 sec^{-1} at 300^oK.

CONCLUSIONS AND RECOMMENDATIONS FOR FURTHER STUDY

Reentry of the space shuttle raises the concentration of nitric oxide by five orders of magnitude in a wake whose initial radius is approximately 8 meters. A relatively persistent wake is formed. A numerical model has been constructed of the eddy diffusive dispersion of the wake. Chemical reactions between wake nitric oxide and the ambient atmosphere have been included, particularly the reaction between nitric oxide and ozone which results in the formation of nitrogen dioxide.

The rate of dispersion of the wake depends on the magnitude of the eddy diffusion coefficient and wind structure. For radial diffusion and an eddy diffusion coefficient of 1100 m^2/sec the centerline nitric oxide concentration is reduced 4 orders of magnitude in 250

seconds. While such high diffusivity may be expected in the extremely turbulent early wake regime, the natural atmospheric diffusivity is considerally less. Thus, Johnson and Wilkins (1966) estimate the upper limit of vertical eddy diffusivity to be approximately 8×10^5 cm^2/sec, i.e. 80 m^2/sec. Since atmospheric eddy diffusivity may be expected to vary by several orders of magnitude we have chosen to consider a vertical diffusivity of 1 m^2/sec as a reasonable lower limit. It must be noted, however, that molecular diffusivity at 70 km altitude is approximately 0.5 m^2/sec. Thus, we may be reasonably confident that our calculation is, indeed, conservative. In the case of 1 m^2/sec the time to reach background can be weeks. Normally strong wind shears are expected. When present these can significantly increase the rate of dispersion of the trail.

As the wake expands atmospheric ozone is converted to molecular oxygen and nitrogen dioxide by nitric oxide. The ozone depletion results in an "ozone hole" in the surroundings of the wake. For a vertical eddy diffusion coefficient of 1 m^2/sec and no wind this ozone hole reaches its maximum size in approximately four hours and collapses again in less than 12 hours. At its maximum the hole is approximately one kilometer wide and 300 meters thick with a length of thousands of kilometers.

The preliminary conclusion is that the transient effects of a reentering shuttle on atmospheric ozone are not very

severe, and do not last much longer than a day. However, large numbers of shuttle flights do pose a potential accummulation of nitric oxide which may seriously affect ozone.

It must be recognized that all computations depend on a number of parameters which are ill-defined. A thorough knowledge of the value of the eddy diffusion coefficient as a function of position and time is essential. The same holds true for wind profiles. The lifetimes of the trail is a sensitive function of these parameters and there are few experimental values. Other quantities such as the ambient distribution of nitric oxide and the ionospheric properties should also be studied in order to better understand the physical and chemical properties of the atmospheric entry altitude regime.

It is recommended that the present computations be expanded to include typical entry trajectories, considered necessary because eddy diffusivity, wind shear and atmospheric chemistry are all altitude dependent. Thus, significant differences in contaminant behavior may be expected. The effect of enhanced ionization resulting from photoionization of the wake should be computed. Nitric oxide production in the extended bow shock should be considered in detail.

A series of nitric oxide release experiments should be conducted in the mesosphere under different atmospheric conditions.

REFERENCES

Ames, W.F., "Numerical Methods for Partial Differential Equations", Barnes and Noble, New York, 1969.

Bailey, A.B., "Turbulent Wake and Shock Shape of Hypervelocity Spheres", AEDC-TR-66-32, Arnold Engineering Development Center, U.S. Air Force.

Bedinger, J.F. and E. Constantinides, "Investigation of Temporal Variations of Winds", GCA-TR-69-3-N, GCA Corporation, Bedford, Massachusetts, August 1969.

Berman, C., and A. Goldburg, "Global Dispersion of Supersonic Transport Exhaust in the Stratosphere", D180-12981-1, Boeing, Seattle, July 1971.

Courant, R. and D. Hilbert, "Methods of Mathematical Physics", Vol. II Partial Differential Equations; John Wiley, New York, 1966.

Goldburg, Arnold, "A Hypersonic Wake Transition Map", AVCO-Everett Research Note 550, July 1965.

Johnson, P.S. and E.M. Wilkins, Correction to 'Thermal Upper Limit on Eddy Diffusion in the Mesosphere and Lower Thermosphere', J. Geophys. Res., 70, 4063, 1966.

Li, Huon, "Hypersonic Non-Equilibrium Wakes of a Slender Body", General Electric Space Sciences Laboratory Report R63SD50.

Slattery, R.E. and W.G. Clay, "The Turbulent Wake of Hypersonic Bodies", Am. Rocket Society Preprint (2673-62) November 1962.

Smith, W., L. Katchen, P. Sacher, P. Swartz and J. Theon, "Temperature, Pressure, and Wind Measurements with the Rocket Grenade Experiment, 1960-1963", NASA TR R-211, October 1964.

Smith, W.S., J.S. Theon, P.C. Swartz, L.B. Katchen and J.J. Horvath, "Temperature, Pressure, Density and Wind Measurements in the Stratosphere and Mesosphere, 1966", NASA-TR-R-288.

Sommerfeld, A., "Partial Differential Equations in Physics", Academic Press, New York, 1949.

Strobel, D.F., "Diurnal Variation of Nitric Oxide in the Upper Atmosphere", J. Geophys. Res., 76, 2441-2452, 1971.

Zimmerman, S. P. and K.S.W. Champion, "Transport Process in the Upper Atmosphere", J. Geophys. Res., 68, 3049-3056, 1963.

APPENDIX A

A one dimensional problem was solved as followed: A length L was considered in which an initial rectangular concentration profile of width $L' = 0.1L$ was located in the center. A history of the centerline concentration as a function of the number of time steps is given in Figure A1.

Figure A2 shows growth of the width at half the centerline concentration where λ is the half width. The asymmetry for long times is believed to be largely due to the way the boundary conditions were chosen, i.e. the concentration at the boundary of the intervals was taken as a fraction of the concentration at a fixed point close to the boundary.

Now, consider application of the calculation to the earth's atmosphere.

From Eq. 8 in the main text we may conclude that

$$t' = n\Delta t' = \frac{n\Delta t}{D} = nr\,\frac{(\Delta x)^2}{D} \qquad \text{(A-1)}$$

where n is the number of computation steps.

At 75 km altitude, Zimmerman and Champion (1963) give an effective diffusion coefficient in the range of approximately 300-2000 m^2/sec. Johnson and Wilkins (1966) deduce 100 m^2/sec. To be conservative, let us choose the lower value of D, i.e. 100 m^2sec.

The numerical solution discussed above shows that it takes 100,000 time steps for the centerline concentration

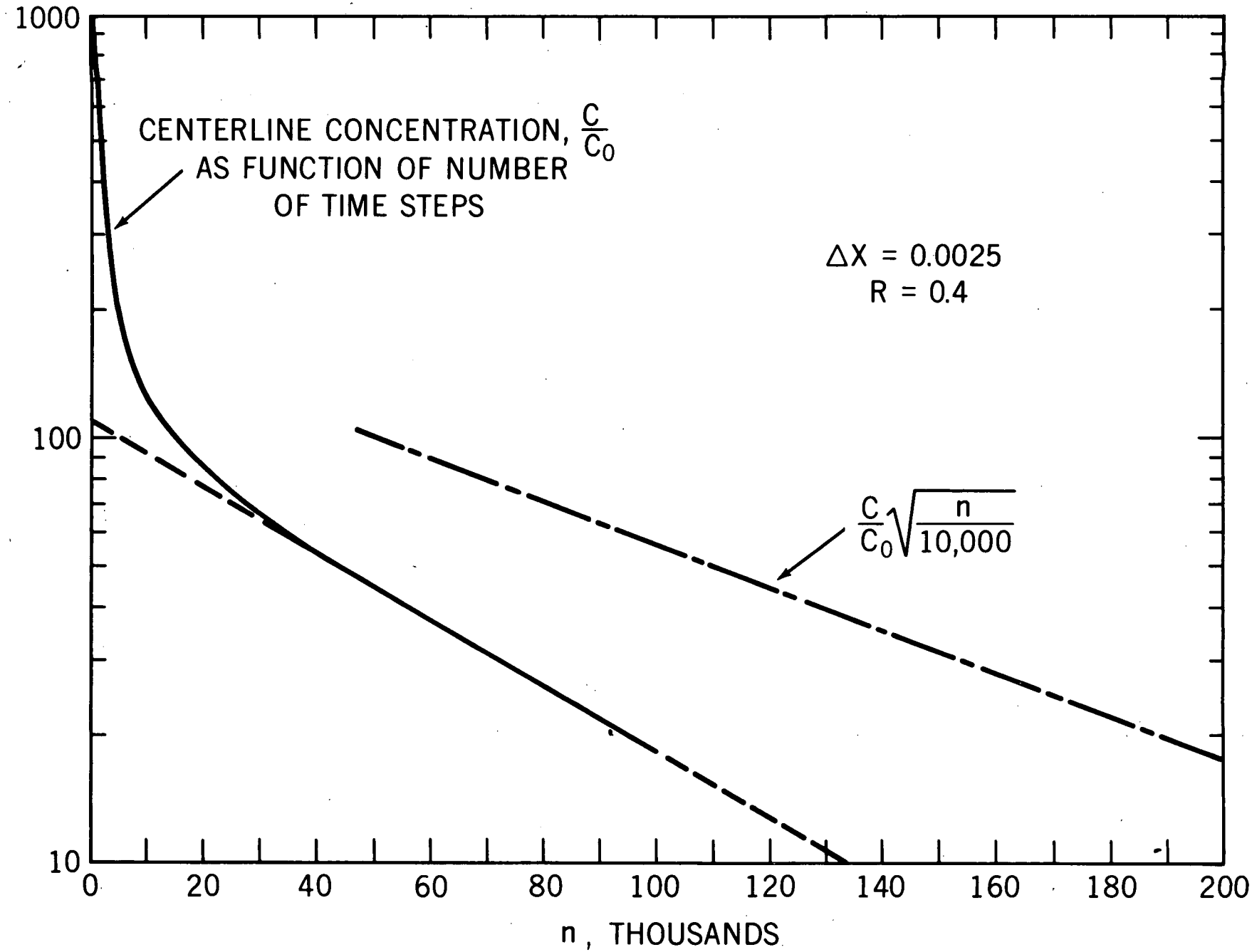
1000
100
10
0
20
40
60
80
100
120
140
160
180
200
n , THOUSANDS
CENTERLINE CONCENTRATION, C/C0
AS FUNCTION OF NUMBER
OF TIME STEPS
ΔX = 0.0025
R = 0.4
C/C0 √(n/10,000)

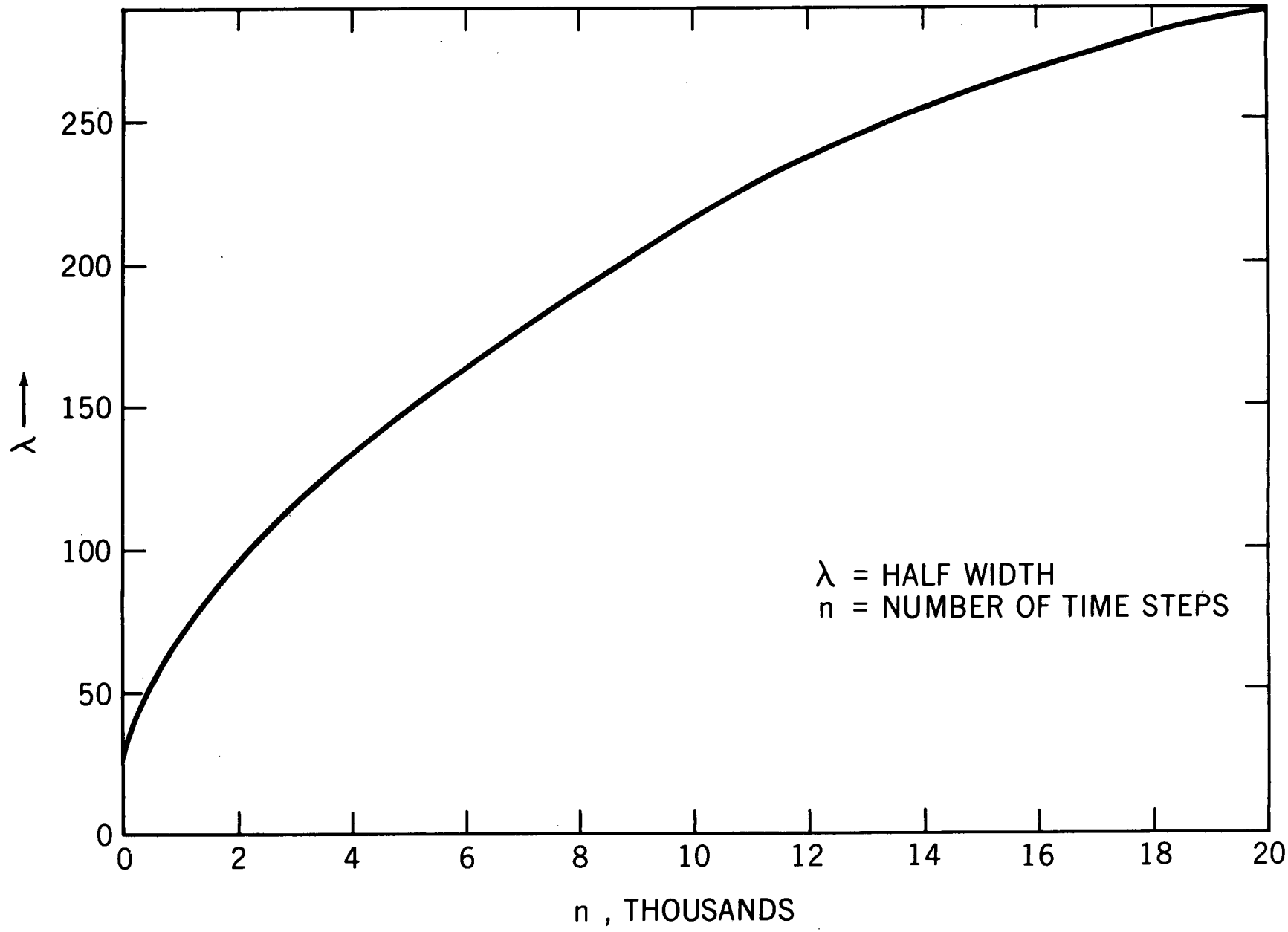

Half width versus number of time steps

to drop from 1000 units to 18 units. Reference to Eq. 4 in the main text shows that concentration appears to the same power on both sides of the equation. Therefore, c may be multiplied by any constant without altering either the differential equation or its solution. Thus the initial 1000 units may be set to any initial concentration c_o, or mole fraction, M_o.

In the numerical computation, the total lateral extent, L, was broken up into 400 intervals, i.e. $\Delta x = \frac{L}{400}$ the ratio, r, was taken as 0.4.

Then, using Eq. A-1: $(\Delta x)^2 = \frac{L^2}{16 \times 10^4}$, giving

$$t' = \left(\frac{n}{10,000}\right)\left(\frac{L^2}{40D}\right) \qquad \text{(A-2)}$$

Equation A-2 may be used to estimate the actual rate of diffusion in the atmosphere. Consider the time, t", required for the centerline concentration to diminish from 1000 units down to 18 units. We know from the computation that this required 100,000 time steps. Thus we have

$$t'' = \frac{L^2}{4D} \qquad \text{(A-3)}$$

It is now a simple matter to estimate t" for various initial widths of the high concentration peak. D is taken as 100 m^2/sec, and t" is given for several L' and L values. L' is the width of the original concentration peak.

L'	L	t''(sec)	t'' (D=100)	t'' (D=300)	t''(D=1000)
4 m	40 m	4	4 sec	1.3 sec	.4 sec
40 m	400 m	400	6.7 min	2.3 min	40 sec
1/2 mile	$8x10^3$m	$16x10^4$	44.5 hours	15 hours	4.5 hours

* D = m^2/sec

A way to check the validity of the above computation is to compare the predictions of Figure A-2 with cloud spreading data measured by Zimmerman and Champion. These authors show that a contaminant cloud at 75 km requires approximately 2000 seconds to grow from 800 meters diameter to 8000 meters diameter. Figure A-3 shows that the width at half maximum grows by a factor of 10 in 13,500 time steps. Equation A-2 may now be used to calculate an effective diffusion coefficient. $L = 10\ L'$, $n = 13{,}500$, $t' = 2 \times 10^3$sec. Thus

$$2x10^3 = (1.35)\ \left(\frac{[8x10^3]^2}{40D}\right)$$

$$\frac{1}{D} = \frac{2x10^3 \times 40}{(8x10^3)(8x10^3)(1.35)}$$

It follows that $D \sim 1080$ m^2/sec.

Now the effective diffusion values quoted by Zimmerman and Champion for 75 km range between 300 and 2000 meters^2/sec, so that the 1100 m^2/sec calculated above is probably more reasonable than the 100 m^2/sec used previously. Nontheless it must be remembered that atmospheric eddy diffusion can easily vary by one, or even two, orders of magnitude depending on the activity of the atmosphere.

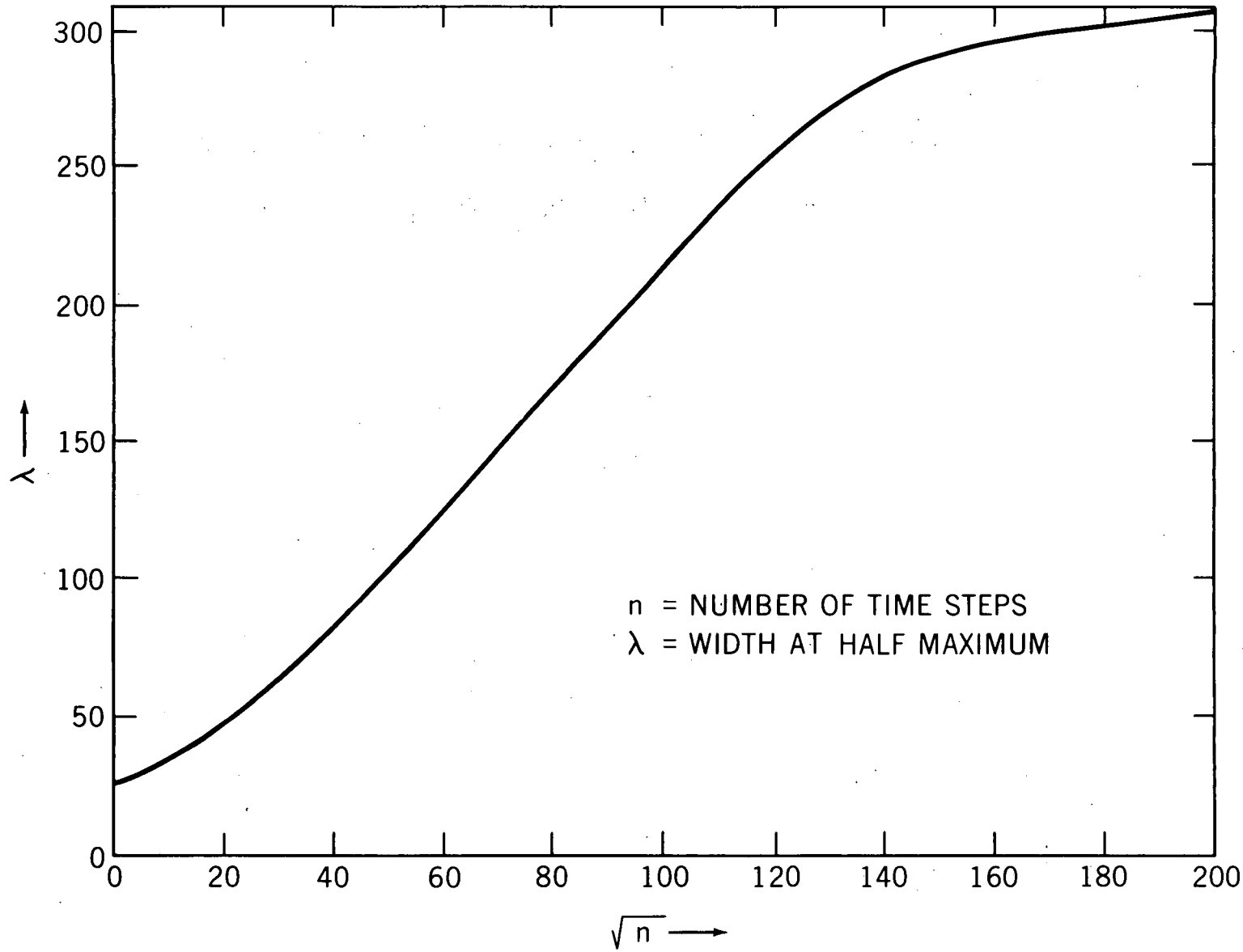

Growth of width at half maximum

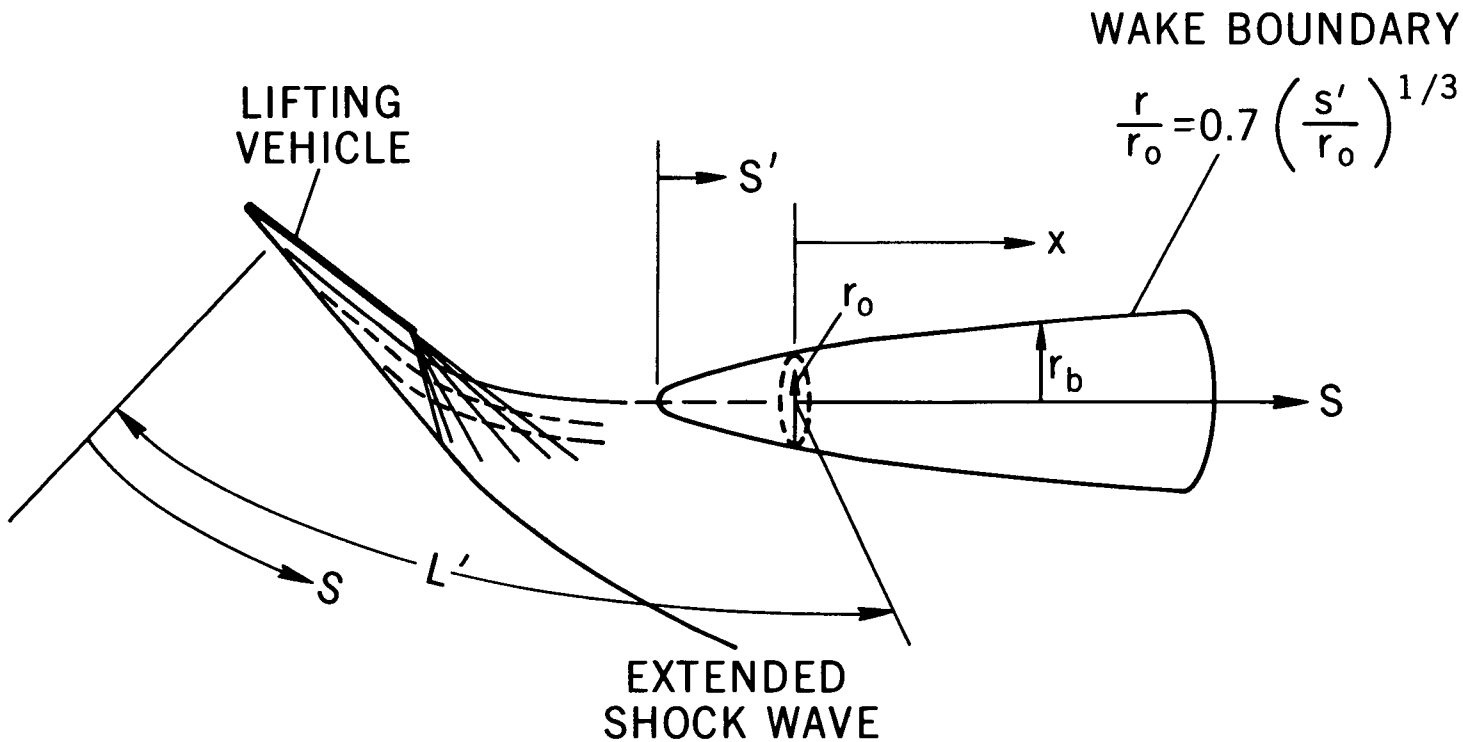

Schematic of two-step flow field model used in computer calculation, from Park (1972)

TABLE I

NEUTRAL REACTIONS

REACTION	RATE
$O_2 + h\nu \rightarrow O + O$	J_{O_2}
$O_3 + h\nu \rightarrow O + O_2(^1\Delta_g)$	J_{O_3}
$O + O_2 + M \rightarrow O_3 + M$	8(-35)EXP(445/T)
$O + O_3 \rightarrow O_2 + O_2(^1\Delta_g)$	5.6(-11)EXP(-2850/T)
$NO + h\nu \rightarrow N + O$	J_{NO}
$N + O \rightarrow NO$	1(-17)
$N_2 + h\nu \rightarrow N + N$	J_{N_2}
$NO + O_3 \rightarrow NO_2 + O_2$	1(-12)EXP(-1200/T)
$N + NO_2 \rightarrow 2\ NO$	6(-12)
$O + NO_2 \rightarrow NO + O_2$	1.66(-11)EXP(-300/T)
$NO_2 + h\nu \rightarrow NO + O$	J_{NO_2}
$NO + NO + O_2 \rightarrow NO_2 + NO_2$	6.61(-39)EXP(526/T)
$NO + O + M \rightarrow NO_2 + M$	3.63(-33)EXP(930/T)
$NO + O \rightarrow NO_2$	4.07(-12)
$NO + O_2 \rightarrow NO_2 + O$	1.58(-12)EXP(-22900/T)
$NO_2 + NO_2 \rightarrow NO + NO + O_2$	6.61(-12)EXP(-13500/T)

LIST OF FIGURES

* U.S. GOVERNMENT PRINTING OFFICE: 1972—735-967/591